(12)

DNA-TR-81-102

FIRESTORMS

G. F. Carrier
F. E. Fendell
P. S. Feldman
TRW Electronics and Defense Sector
One Space Park
Redondo Beach, California 90278

15 April 1982

Technical Report

CONTRACT No. DNA 001-81-C-0111

THIS WORK WAS SPONSORED BY THE DEFENSE NUCLEAR AGENCY
UNDER RDT&E RMSS CODE B345081466 G54CAXYX00001 H2590D.

Prepared for
Director
DEFENSE NUCLEAR AGENCY
Washington, DC 20305

UNCLASSIFIED

SECURITY CLASSIFICATION OF THIS PAGE (When Data Entered)

REPORT DOCUMENTATION PAGE		READ INSTRUCTIONS BEFORE COMPLETING FORM
1. REPORT NUMBER DNA-TR-81-102	2 GOVT ACCESSION NO. AD-A131 147	3 RECIPIENT'S CATALOG NUMBER
4. TITLE (and Subtitle) FIRESTORMS		5 TYPE OF REPORT & PERIOD COVERED Technical Report
		6. PERFORMING ORG. REPORT NUMBER 38163-6001-UT-00
7 AUTHOR(s) G. F. Carrier (Harvard University, Cambridge, MA) F. E. Fendell P. S. Feldman		8. CONTRACT OR GRANT NUMBER(s) DNA 001-81-C-0111
9 PERFORMING ORGANIZATION NAME AND ADDRESS TRW Electronics & Defense Sector One Space Park Redondo Beach, California 90278		10. PROGRAM ELEMENT, PROJECT, TASK AREA & WORK UNIT NUMBERS Task G54CAXYX-00001
11. CONTROLLING OFFICE NAME AND ADDRESS Director Defense Nuclear Agency Washington, D.C. 20305		12. REPORT DATE 15 April 1982
		13. NUMBER OF PAGES 84
14. MONITORING AGENCY NAME & ADDRESS(if different from Controlling Office)		15. SECURITY CLASS. (of this report) UNCLASSIFIED
		15a. DECLASSIFICATION/DOWNGRADING SCHEDULE N/A since UNCLASSIFIED

16. DISTRIBUTION STATEMENT (of this Report)

Approved for public release; distribution unlimited

17. DISTRIBUTION STATEMENT (of the abstract entered in Block 20, if different from Report)

18. SUPPLEMENTARY NOTES

This work was sponsored by the Defense Nuclear Agency under RDT&E RMSS Code B345081466 G54CAXYX00001 H2590D.

19. KEY WORDS (Continue on reverse side if necessary and identify by block number)

Fire	Natural Convection
Firestorms	Nuclear Weapon Effects
Firewhirl	Plumes

20. ABSTRACT (Continue on reverse side if necessary and identify by block number)

Firestorms have arisen from the merger of fires from multiple simultaneous ignitions in a heavily fuel-laden (urban) environment. Within an hour surface-level radial inflow from all directions sustains a large-diameter convective column; typically, the firestorm reaches peak intensity in a couple of hours, with inflow speeds inferred to attain 25-50 m/s and with the plume reaching 10 km (e.g., Hamburg, Dresden, Hiroshima). Winds associated with the nonpropagating holocaust relax to ambient in six-to-nine hours, with often 12 km^2

DD FORM 1 JAN 73 1473 EDITION OF 1 NOV 65 IS OBSOLETE

UNCLASSIFIED

SECURITY CLASSIFICATION OF THIS PAGE (When Data Entered)

20. ABSTRACT (CONTINUED)

reduced to ashes. Here the firestorm is interpreted to be a mesocyclone (rotating severe local storm), with exothermicity from combustion (rather than condensation of water vapor) supporting convectively induced advection. The rapid swirling of the surrounding air results in reduction of entrainment into the plume, such that the mass flux ascending in the buoyant plume is furnished entirely by a near-ground layer with large radial inflow. Integral treatment of a convective column over a maintained heat source in the absence of a cross-wind is generalized to include (1) reduction of entrainment with swirling; (2) stratification of the ambient that varies with altitude; and (3) time evolution based on spin-up under conservation of angular momentum, incorporating large radial pressure gradient. Only exceedingly large heat release rate sustained over a concentrated area, in the presence of a very nearly mechanically unstable atmospheric stratification, is consistent with onset of vigorous swirling on the scale of two hours.

PREFACE

The authors are grateful to R. Flory, M. Frankel, and T. Kennedy for the opportunity to pursue this investigation; to Lauren Hall for preparation of the manuscript and to Asenatha McCauley for preparation of the figures. This work was supported under Defense Nuclear Agency contract DNA001-81-C-0111.

TABLE OF CONTENTS

TABLE OF CONTENTS (Continued)

LIST OF ILLUSTRATIONS

1. INTRODUCTION

1.1 Preliminary Comments

If the standard reference The Effects of Nuclear Weapons (Glasstone and Dolan, eds. 1977) is consulted, it is readily ascertained that the blast and radioactive fallout consequences of a nuclear event have been far more extensively investigated than the incendiary consequences. Yet, "... there is good reason to regard the Hiroshima and Nagasaki bombs as largely, and perhaps even primarily, incendiary weapons, and only secondarily as blast and radiation weapons" (SIPRI 1975, p. 163). This investigation is aimed at elucidating the nature and causes of a particularly virulent and long-lived uncontrolled burning that occurred in the aftermath of the atomic bombing of Hiroshima in World War II, a firestorm. However, that firestorm began about a half hour after the explosion and persisted for about six hours, and thus plausibly is not uniquely associated with the nuclear origin; in fact, massive simultaneous use of conventional incendiary and high-explosive bombs on urban targets in World War II engendered events of wind-aided fire spread comparable in duration, scale, and intensity to that following the atomic bombing of Nagasaki, and, more relevantly, (on a few rare occasions) engendered firestorms comparable in duration, scale, and intensity to that following the atomic bombing of Hiroshima[#] (SIPRI 1975).

Thus, in this investigation, an extensive, considered (but not exhaustive) review of the literature concerning firestorm-like events is undertaken to motivate the basis of important postulations that underlie the quantitative modeling. For reasons already set forth, firestorm-like events arising in the context of natural disasters, as well as in the context of military weapons of mass destruction, are to be included in the review. While the point can hardly be overemphasized, for avoidance of reiteration, suffice it once and for all to state that the "data base" for a theoretical study of the firestorm currently consists to very small extent of objective, verifiable, quantitative measurement, and to very

[#]It has been estimated that the fire damage to structures and buildings at Hiroshima could have been produced by about 10^6 kg of incendiary bombs distributed over the city (Glasstone and Dolan, eds. 1977).

large extent of observational, nonreproducible, qualitative description. Thus, albeit with reservation, necessarily advantage must be taken of unconventional sources.

1.2 A Thesis Concerning the Firestorm

> About 20 minutes after the detonation of the nuclear bomb at Hiroshima, a mass fire developed showing many characteristics usually associated with fire storms. A wind blew toward the burning area of the city from all directions, reaching a maximum velocity of 30 to 40 miles per hour about 2 to 3 hours after the explosion, decreasing to light or moderate and variable in direction about 6 hours after... The strong inward draft at ground level was a decisive factor in limiting the spread of fire beyond the initial ignited area. It accounts for the fact that the radius of the burned-out area was so uniform in Hiroshima and was not much greater than the range in which fire started soon after the explosion. However, virtually everything combustible within this region was destroyed. (Glasstone and Dolan, eds. 1977, p. 304)

> In a firestorm many fires merge to form a single convective column of hot gases rising from the burning area and strong, fire-induced, radial (inwardly directed) winds are associated with the convective column... Apart from a description of the observed phenomena, there is as yet no generally accepted definition of a fire storm. Furthermore, the conditions, e.g., weather, ignition-point density, fuel density, etc., under which a fire storm may be expected are not known. Nevertheless, based on World War II experience with mass fires resulting from air raids on Germany and Japan, the minimum requirements for a fire storm to develop are considered by some authorities to be the following: (1) at least 8 pounds of combustibles per square foot of fire area, (2) at least half of the structures in the area on fire simultaneously, (3) a wind of less than 8 miles per hour at the time, and (4) a minimum burning area of about half a square mile. (Glasstone and Dolan, eds. 1977, pp. 299-300)

Kerr (1971) ascribes the origin of the term firestorm to a German reporter in World War II who noted similarities between rainstorms and some fires. In a meteorological context, storm suggests cyclonic winds about a center of low surface pressure, with precipitation from convectively induced advection (i.e., from buoyancy-caused ascent of warm and/or moist air leading to radial influx, under continuity, and possible attendant spin-up, under conservation of angular momentum associated with earth rotation or some locally enhanced level). Thus, the term firestorm suggests a mesolow in which the exothermicity of combustion, as distinguished from the condensation of water vapor, induces free convection, and hence associated movement of air closer to the axis of rotation, such that the air spins more rapidly as the radial distance to the

axis is decreased.[#] In fact, it is interesting that, just as firestorms are exceptional events relative to the total number of large urban and wildlands fires, mesolows (thunderstorms with organized rotation, also referred to as tornado cyclones and supercells) are uncommon relative to the total number of thunderstorms, but occur on the horizontal scale of several kilometers and persist up to about six hours (Brandes 1978).[§] Furthermore, recent analytical and numerical investigation of the near-surface inflow layer (near the center of a vigorously rotating airmass over a fixed flat surface) has shown that strong, purely swirling motion is altered to equally strong, purely radial influx near the ground, though immediately at the ground the no-slip constraint holds (Carrier 1971a; Burggraf et al 1971; Carrier and Fendell 1978). Hence, the observation at low levels of appreciable radial influx from all directions toward the base of the centrally sited convective column corroborates, rather than contradicts, the primarily rotating nature of the bulk of the air motion. In that mesocyclone cyclogenesis from the ambient angular momentum levels of the earth requires that advective buildup persist for an hour or more, it appears consistent that significant convection must persist for a significant fraction of an hour over an adequate surface area for a firestorm to arise (Davies-Jones and Kessler 1974; Long 1967). Diffusional relaxation mechanisms counter the spin-up (Dergarabedian and Fendell 1974), such that usually the magnitude of organized swirling is either modest or nil; the firestorm is the

---

[#]Ebert (1963) refers to the firestorm in Hamburg, Germany on 28 July 1943 as a "heat cyclone".

[§]The criterion of low ambient wind for the onset of a firestorm raises several points. Tropical cyclones form in environments in which there is little vertical wind shear to cause ventilation, i.e., in environments in which wind parallel to the surface of the ocean varies modestly in magnitude and direction with altitude above the surface, so that a vertical column of rising lower-density air creates surface-level horizontal pressure differences from hydrostatic considerations (Fendell 1974). Strong vertical wind shear could disperse the convective column so that no appreciable surface-level pressure difference would arise, and an organized airmass with lower-tropospheric rotation would not ensue. However, for the more relevant scale of a midlatitudinal thunderstorm, vertical wind shear is usually a prerequisite for genesis; whether appreciable vertical wind shear typically precedes formation of a mesolow (a rotating thunderstorm, that tends to veer to the right of mean winds) is less clear. In any case, the eight-miles-per-hour constraint on surrounding winds seems a vague (and perhaps invalid) precondition.

exceptional event. Further, just as the mesolow is characterized by towering cumulonimbi ascending through the depth of the troposphere to the tropopause, so the firestorm is reported to be characterized by a convective column rising to unusual altitudes, e.g., 10,000-13,000 m at Hamburg. Finally, chance advent of a cyclonic, low-pressure atmospheric system at the site of convective activity (e.g., from a fire) is conjectured to lead to locally enhanced background circulation levels, such that spin-up time-span is reduced (Taylor and Williams 1968).

Thus, the thesis here is that the firestorm is aptly named: it is a fire generated rotating thunderstorm. By this thesis, any investigation of the generating conditions, mature-stage properties, and decay of a firestorm that omits consideration of rotation (i.e., conservation of angular momentum) would seem to be so incomplete as to be inadequate. If this thesis be valid, significant insight into the firestorm is to be gained from known properties of atmospheric circulation systems generically referred to by meteorologists as severe local (convective vortical) storms; meteorological analogue is to be returned to frequently throughout this development.

There are already in the literature many allusions to the parallel between firestorms and tropospheric storms in the superficial sense of strong convection accompanied by strong surface winds. However, the authors are aware of at least two qualitative descriptions of the firestorm that draw attention to the likely pertinence of the dynamic characteristics of a rapidly rotating airmass above a relatively fixed flat surface plane (Emmons 1965; Long 1967). In fact, some remarks by Emmons (1965, p. 959) are well worth quoting:

> No general discussion of fire problems is complete without a reference to the very severe wartime fires of Hamburg and several other cities in which a number of square miles were burned out in some six hours of most violent fire. Winds grew to hurricane level, blowing everything loose into the heart of the fire. Needless to say, exact measurements are not available on winds, temperature, fire-plume characteristics, upper-level winds, stability of the atmosphere, and many other details which would need to be measured if reasonably complete understanding of the events were to be attained.
>
> One thinks at first that the rising plume of a large-area fire might give rise to winds of the required magnitude. However, estimates do not seem to bear this out, since by mixing with

> cool air the density of the plume rises too fast to maintain the required buoyancy. If, however, the atmosphere were unstable at the time of the fire, the fire plume might be enhanced in altitude and buoyancy by contributions from the unstable air. This explanation is difficult to check since the velocities encountered in Hamburg were on the upper edge of any that nature ever produces.
>
> An alternative explanation supposes a gigantic fire whirl. If there were sufficient wind shear at the time of the fire, a fire whirl of enormous size might develop. Several qualitative effects of such air circulation are noteworthy. Since the air outside of the fire plume is rotating rapidly while that inside is not, the normal plume mixing process is prevented by centrifugal force, the plume stays hot to far higher altitudes and hence the high buoyancy required to produce high velocities is available.
>
> Furthermore, the rotating air high above the ground produces a balancing radial pressure gradient. This radial pressure gradient imposed upon the relatively noncirculating air near the ground drives the latter toward the center of the fire. Thus the air supplied to the fire comes from a layer near the ground and the resultant winds are far from tangential to circles around ground zero. Thus the fact that trees blown down in Hamburg did not show a distinct tangential air motion is not contradictory to the existence of a fire whirl a mile or more high.

Nevertheless, neither of these authors quantitatively develops the point; indeed, Morton (1970) reports sufficient scepticism concerning the above-stated thesis that a somewhat detailed review of the observational literature on firestorms seems appropriate (Section 2).

Both this review, and the subsequent quantitative modeling of the firestorm, is motivated by the particular severity of this fire within its periphery; the firestorm may well be the "worst-case scenario" for a free-burning fire. Furthermore, the well-known propensity for long-range, spotting-type (discontinuous) spread of free-burning fire via firebrands in the event of firewhirls (Graham 1955; Countryman 1971; Lee and Hellman 1974) suggests that the spatially confined character of most firestorms may have exceptions.

1.3 Distinction of the Firewhirl and the Firestorm, and Their Occurrence in Wildlands

In a severe convective vortical storm of the troposphere, swirling may exist simultaneously on several lateral scales. The overall thunderstorm may possess a Rankine-vortex-type swirl profile (near-axis rigid-body rotation, merged to potential-vortex form far from the axis of rotation), with peak swirl of roughly 20 m/s occurring several kilometers from the axis of rotation; this scale of swirling may persist for six hours or so. Perhaps one-quarter, perhaps even a higher fraction, of mesolows engender one or more severe tornadoes. A moderate tornado persists for about ten minutes, has peak swirl speed of barely 50 m/s, and wreaks damage over a path (say) a hundred meters in width and a couple of kilometers in length. In contrast, a severe tornado persists for an hour or so, has peak swirl of a little over 100 m/s (relative to the axis of rotation, which itself can translate up to 40 m/s), and wreaks damage over a path a half-kilometer wide and 160 km long. (Normally the damage is discontinuous owing to topography, transient variations in tornado strength, etc.) The point is that the horizontal scale of the tornado is clearly smaller than that of the spawning mesolow (cumulus scale as distinct from mesoscale). But the tornado is not a steady axisymmetric system, but itself consists of several "large-scale substructures" referred to as satellite or suction vortices, shorted-lived whirls; these translate around the tornado axis in an annulus roughly circumscribed by the airmass referred to commonly as the tornado. The horizontal spatial scale of a satellite vortex is perhaps an order of magnitude smaller than that of the tornado. Analogously, typhoons (which can extend to a radius of 800 km in the western North Pacific Ocean) can encompass thunderstorms, and certainly include in the eyewall annulus a high density of cumulonimbi, towering rainclouds in whose inner core saturated air rapidly ascends with very little dilution from mixing with cooler, drier midtropospheric air (probably because of the appreciable swirling of the local environment). Again, in the atmosphere, unconstrained by lateral boundaries, swirling can exist on several horizontal spatial scales, often simultaneously.

Since the laboratory experiments of Byram and Martin (1962), systematic studies of the tall fire-generated whirlwind have been carried out; the

firewhirl is a vortex of the generic category that includes waterspouts, dustdevils, whirls near volcanic eruptions (Thorarinsson and Vonnegut 1964; Thorarinsson 1966), tornadoes, etc. Such firewhirls tend to form sometime after initiation, near the peak convective activity and after convectively induced advection has allowed a sufficient time interval for spin-up. A particularly-well-documented firewhirl of three-minute duration occurred on 7 March 1964 northwest of Carpenteria in Santa Barbara County, California, during a fire in heavy brush on steeply sloped hills; yet, even in this event, one author (Lohneiss 1966) characterized the prevailing wind as northwesterly and under 5 m/s, whereas others (Pirsko et al 1965) write of towering cumulonimbi in conditionally unstable air and of winds of 9-10 m/s (with gusts of 15 m/s). Graham (1952) describes an intermittently detectable firewhirl of ten-minute duration, formed in convectively unstable air by the interaction of opposing winds near a ridge crest, on 23 August 1951 at the Vincent Creek fire in southwest Oregon. Hundreds of firewhirls, some of tornadic strength, were engendered over a 27-hour period on 7-8 April 1926 when lightning ignited oil-storage containers south of San Luis Obispo, California, the resulting flames rising 330 m into the air (Hissong 1926).

However, interest here centers on longer-lived, larger-horizontal-scale fire-associated whirls; there are general statements (Brown and Davis 1973; Lyons 1978) that firestorms can arise in very exceptional wildlands fires (as opposed to urban fires), but there is little documentation. Graham (1955) notes a firewhirl formed on a lee slope on 20 July 1951 at 1600 PST in the North Oregon Coast Range that persisted for two hours, had a diameter of 400 m and height of 830 m, and moved logs 75 cm x 10 m. Taylor et al (1973) report that an hour after onset of a bush-fire on a flat plain (5 kg/m^2 of fuel loading) south of Darwin, Australia on 10 September 1971 in hot dry air[#], the plume over an area 2 km x 3 km rose from

[#]Taylor and Williams (1968) point out that thunderstorm-prone conditions typically entail conditionally unstable air owing to the presence of appreciable water vapor in the lower troposphere. In contrast, hot, dry, nearly autoconvectively unstable air, such as that conducive to dustdevil formation, is compatible with fire blow-up. In fact, the lapse rate to 6000 m was constant at 0.006 K/m in the Darwin fire described in the main text, whereas the dry adiabatic lapse rate is 0.01 K/m. In July 1943 in Hamburg hot dry light-wind conditions prevailed, with a nearly dry-adiabatic lapse to 3,300 m, at the time of the firestorm. However, firestorms have also occurred under different meteorological conditions (see below).

3000 m to 5800 m in 15 min; these authors suggest that a reduction in entrainment seems required to explain the ascent. As is discussed below, ascent in a rotating environment is one of the very few plausible mechanisms for reduction in entrainment.

No discussion of wildlands firestorms is complete without reference to the spectacular run of the Sundance fire in the Pack River basin in northern Idaho on 1 September 1967, during hot dry windy weather. In nine hours under sustained winds of 22 m/s, the fire advanced 14 km and burned out 200 km^2. At peak intensity, winds in the fire are estimated to have reached 50 m/s, and numerous small-diameter dustdevils and firewhirls were observed. The energy release rate is estimated at 4.98×10^8 kW (the total loading is estimated to have been as high as 6.2 kg/m^2 of a fuel estimated to yield 2×10^7 J/kg if completely dry) (Anderson 1968). Whether very-large-scale rotation developed during this interval remains a subject of speculation.

1.4 Experimental Firestorms

Since the laboratory experiments of Byram and Martin (1962), measurement of properties of firewhirls has been a widely pursued activity in the discipline of free-burning-fire research (e.g., Emmons 1965; Ying 1965; Emmons and Ying 1967). However, since atmospheric stability, large-scale turbulent diffusion, and conceivably radiative transfer enter significantly in firestorms, large-scale experiments seem required. Perhaps the most noteworthy of these involve the so-called Meteotron at the Centre de Recherches Atmospheriques Henri Dessens on the plateau of Lannemezan, 600 m above sea level and 20 km north of the Central Pyrenees Mountains of France (Dessens 1962, 1964; Benech 1976; Church et al 1980). In the past two decades hundreds of quarter-to-half-hour experiments have been conducted with scores of fuel oil burners in various geometric configurations; the most recent tests have entailed 105 burners, arranged 4 m apart in a three-armed spiral pattern within an area of 140 m x 140 m, each burner consuming diesel oil at the rate of 1 m^3/hr so that the total energy release rate is of 1000 MW.[#] Each burner produces a flame five-to-ten meters long, one meter in diameter, the flame plumes from each burner merging into a single buoyant plume about 10-20 m above ground level. Each of the electrode-ignited burners consumes 600 kg of fuel oil per hour, but combustion is incomplete (flame temperature is 1500 K) so thick black smoke permits visualization of the ascending column. The temperature discrepancy between the inside of the plume and the surrounding air is typified (Benech 1976) as about 100 K maximum, reduced to 50 K at 10 m (where the plume is roughly 40 m in horizontal scale), and less than 10 K at 100 m; vertical speeds reach 8 m/s but are reduced to about 3 m/s at 10 m; the plumes rise to heights between about 500 and 1500 m.

Short-lived tall narrow dustdevil-like vortices are occasionally observed seven minutes or more after experiment initiation; these may have a diameter of up to 2 m and persist several minutes. However, on two

[#]A typical thunderstorm has areal scale of 10 km^2, persists an hour, and is characterized by 5 x 10^4 MW; the Darwin bushfire discussed in Section 1.3 is characterized by 50 km^2, several hours duration, and 10^5 MW; the San Luis Obispo oil-tanks fire, by 3.2 km^2, many-hours duration, and 700 MW; Surtsey volcano, by 1 km^2, several-months duration, and 10^5 MW (Hanna and Gifford 1975).

occasions (31 August 1961 and 8 July 1978) the entire lower portion (at least) of plume has gone into rotation as a whole, so that columnar vortex of 40 m diameter has formed. On the earlier occasion (with the temperature 303 K, relative humidity 65%, wind at about 1.3 m/s, and an unstable layer persisting up to 2 km), the organized whirling began 15 min after experiment initiation and lasted 3-4 min. The flames inclined toward the plume center at 45°, the wind being strong enough to blow out three burners. On the later occasion, a rawinsonde taken four km away one-half hour after the experiment indicated a superadiabatic surface layer (92.8-94.2 kPa) and a capping inversion (83-88 kPa), with wind at 6 m under 2 m/s.

Thus, on very rare occasions, characterized by calm but unstable atmospheric conditions, onset of relatively large-scale organized rotation was observed long enough after initiation of convection for spin-up to have occurred. These observations do not seem inconsistent with the thesis that the more common firewhirl and the less common firestorm represent two different lateral scales of organized rotation in chemical-exothermicity-engendered convective atmospheric flows.

1.5 Urban Firestorms from Natural Catastrophes

Atallah (1966) has conjectured that the Chicago, Illinois fire of 8-10 October 1971, in which 8.6 km^2 and 17,450 buildings were destroyed, was a firestorm, but it seems far more likely that wind-aided fire spread was entailed. However, the Great Kanto Earthquake just before noon on 1 September 1923 [rated 8.3 on the Richter scale, the same as the San Francisco quake of 1906, with 8.9 about the highest reading ever recorded (Busch 1962)], centered in Sagami Bay (off the east coast of Honshu in the Japanese chain), engendered a tsunami and coincided with a typhoon; almost exactly twenty-four hours later a second shock as strong as the first occurred. This confluence of disasters was aggravated by the fact that the first quake produced 134 separate ignitions within an hour (of which 100 were not extinguished) in Tokyo, and 208 ignitions in Yokohama; 18.2 km^2 and 85% of the structures in Tokyo (about 96 km from the epicenter) were burned, and 7.8 km^2 and 60% of the structures in Yokohama (about 80 km from the epicenter) were consumed. The fires raged for 40 hours (until 3 a.m. on 3 September) in Tokyo; the Yokohama blaze had died down about twelve hours earlier. Since a fairly well-documented gigantic firewhirl [firestorm (?)] was part of this catastrophe, the event is to be examined here in some detail.

Japanese homes at this time were made of light strips of resinous wood, with or without a thin plaster covering, the partitions being sliding wood-and-paper panels. Floors were covered by mats of rice-straw, roofs were of light tile, and mortise (not nails) joined timbers. This heavily wooden construction was crowded together, separated only by very narrow thoroughfares (Busch 1962)[#]. Coal, gas, or charcoal braziers, lit for the noon meal, were left unattended; tipping by the quake spilled live coals on inflammable material -- this is accepted as the explanation for half the fire starts, with chemicals, explosives, and firebrands being cited as the source of the other half. Gas-main and electrical-power-line breaks and the involvement of oil-and-coal-storage sites enhanced the fire spread.

[#]Tokyo had had, during a 250 year interval, fifty fires greater in area, and far more destructive in human life, than the Great Fire of London (1966), which was the worst fire-related catastrophe in the Occident during the same era (Busch 1962).

In a scenario foreboding of later urban holocausts engendered by mixed incendiary and high-explosive bombing, broken water mains, collapsed fire stations, impassable roads and buried fire engines precluded effective fire-fighting (Davison 1931).

Japan experiences landfall of about a dozen typhoons annually, and the coincident churning of a typhoon 160 km north of Tokyo at noon on 1 September complicates discussion of the ambient atmospheric state. The cyclone had passed over the islands of Kyushu and Shikoku (to the southwest of Honshu) on 30 August, and on 1 September moved across the central portion of Honshu, from southwest to northeast in direction. A secondary cyclone approached Tokyo from the south, and also travelled northward, then eastward across the portions of Honshu near Sagami Bay and Tokyo Bay on 1 September (Davison 1931)[#]. Thus strong winds and rainshowers marked the early morning hours of 1 September, though the weather was fair, clear, and calm by 10 a.m., Tokyo being sunny and warm (300 K) while the premier commercial port of Yokohama was cooler. However, winds from the south increased from 12 m/s to 22 m/s during the afternoon of 1 September; around 6 p.m. the winds came from the west and later from the north, and increased to 26-27 m/s by 11 p.m. (Bureau of Social Affairs 1926). The exceptionally strong winds were able to lift galvanized-iron sheets and baulks of timber. Wind-aided flame extended 100 m into the air, and changes in wind direction caused the fire to back over previously burned area. The upward convective currents of smoky air formed tall cumulonimbus clouds owing to the condensation of water vapor released by combustion.

Numerous firewhirls (some uprooting trees 40-50 cm in diameter) were observed in both Yokohama and Tokyo during the course of this urban fire, perhaps at its time without historical precedent. However, interest here centers on a flaming cyclone, estimated to be swirling counterclockwise at 70-80 m/s, that formed at 4 p.m. on 1 September at the Sumida River; this vortex, which reportedly had the sound of a waterfall, lifted small boats

[#]Taylor and Williams (1968) cite the Hellgate Fire in a mountainous area of the George Washington National Forest in western Virginia of 18-19 April 1965 as a case of a fire occurring in the warm sector of an extratropical cyclone (winds of 8-10 m/s, with gusts of 15; airmass absolutely unstable to 1500 m, and favorable for convection to 3,300 m), with significant firewhirl and spotting-type-spread activity resulting.

up to height of five meters out of the water and drew the waters of the river 15 m into the air (Busch 1962). It then moved toward the Military Clothing Depot, an open area of 66,000 m^2 in Honjo-Fukagawa Ward on the east bank of the Sumida. Bricks, timbers, carts, human beings, etc., were lifted skyward by the swirling inferno, and within two hours, almost all of the estimated 40,000 inhabitants who had sought refuge in this cleared area were dead of suffocation and/or burns (Bureau of Social Affairs 1926). The roaring, swirling pillar of fire (characterized by 300 m diameter at the base, and 100-200 m height) moved at up to 10-15 m/s and persisted for <u>at least</u> 35 min. It flattened trees in its path and tore a 60 cm-diameter pasania tree out of the ground. Between one-half and one-third of all the fatalities associated with the entire forty-hour holocaust in Tokyo were associated with this one event, that appears to justify classification as an urban firestorm generated by natural catastrophe.

2. MASSIVE INCENDIARY BOMBING SINCE 1940 AND FIRESTORM OCCURRENCE

2.1 Incendiary Raids on Germany in World War II

Kilogram for kilogram, incendiary bombs were approximately five times as effective in causing damage on German cities in World War II as high-explosive bombs. Four-fifths of the damage to English and German cities was owing to fire as opposed to blast (Bond, ed. 1946). Thus, whereas incendiaries constituted 25-30% of the bomb loads early in the war, they constituted 70% later in the war (SIPRI 1975); the 30% of high-explosive bombs retained not only scattered debris and made internal ignitions easier, but also precluded countermeasures by breaking water mains, blocking streets, destroying firefighting equipment, and forcing firefighting personnel to cover.

Forty-nine of the larger German cities were attacked in incendiary raids during World War II and 39% of the dwelling units in these cities were destroyed or seriously damaged; but firestorms occurred only in Hamburg (27-28 July 1943), Kassel (22-23 October 1943), Darmstadt (11-12 September 1944), and Dresden (13-14 February 1945), according to the U.S. Strategic Bombing Survey (SIPRI 1975). While there may have been one-or-two additional firestorm events[#], clearly the firestorm was an exceptional occurrence[§]. Irving (1965) notes that firestorms occurred after a change in bombing tactics: instead of successive waves dropping bombs along a few diagonals across the target city, a simultaneous saturation (carpet-) bombing of a specific sector was attempted. Nevertheless, firestorm events never occurred in Munich or Berlin, despite very heavy incendiary bombing;

[#]For example, Broido (1960) notes that, after aereal bombardment, Leipzig experienced a convection column extending to 3,900 m, a 15 m/s radially inward wind at sites 4 km from the fire center, and winds in excess of 34 m/s close to the fire center. Irving (1965) notes that 7.7×10^5 kg of bombs dropped on Brunswick on 14-15 October 1944 in a 40-min raid destroyed 2.7 km^2 of the 5.6 km^2 constituting the central city, with much firewhirl activity. The fire continued for six days. At its most intense stage, it may have been of firestorm character.

[§]The German Luftwaffe often employed incendiaries as 60% of its bomb load in raids on English targets in 1940-1941. Irving (1965) states that only on one occasion during a neap tide of the Thames River (so the hoses of the London fire brigades could not reach the water), did an unusually heavy German incendiary attack on London almost initiate a firestorm.

prevalence of stone and brick walls and broad avenues perhaps precluded merging of smaller fires.

American incendiary bombs included clusters of 110 1.8-kg bombs (0.5 kg of magnesium in a 53 cm long tube, with a thermite igniter and a 0.9 kg iron head for penetration of roofs and floors), rated at 1.4×10^4 kJ; clusters of 38 2.8-kg bombs (containing 1.2 kg of gelled gasoline), rated at 4.6×10^4 kJ; a 32 kg bomb (containing 18 kg of combustible-oil mix), rated at 7×10^5 kJ; and a 213 kg bomb (containing 79 kg of combustible-oil mix), rated at 2.32×10^6 kJ (Bond, ed. 1946). English incendiary bombs included a 1.7 kg bomb (containing 250 g of combustible mixture: 36% gasoline, 20% aluminum, 10% crude rubber, 3% oxide, 5% binder, etc.) and 14-kg bomb [containing 3.5 liters, 88% incendiary oil (benzene), 10% crude rubber, and 2% white phosphorus] (SIPRI 1975); these two bombs were often used by the Royal Air Force in equal proportion by weight (Bond, ed. 1946). Omissions from this inventory list generally consist of larger devices that were regarded as less effective (Bond, ed. 1946).

Probably the two most devastating and closely studied firestorm events concern Hamburg and Dresden, and these are now examined individually.

2.2 Hamburg

Hamburg was the second largest city of the German Reich and was the target of 137 raids before July 1943, the last heavy attack occurring on 26 July 1942. Thus, special effort was expended on civil defense, including reinforcement of basement shelters, sand and water storage, flame-retardant treatments, clearing of attic space, and strengthening of roofs. However, defenses were unable to cope with four enormous raids during the ten-day period from 24 July 1943 to 2 August 1943, in which almost 8×10^6 kg of bombs (half of them incendiaries) were dropped. The city was 55-60% destroyed, and 75-80% of this was attributed to fire; in the aftermath, soot, dust, and smoke formed a thick blanket over the entire city. Included in the burning was probably the best-documented firestorm of World War II, and thus the meteorological, structural, and aerothermochemical aspects of the event are here discussed in some detail.

At the core of Hamburg, there were three-to-five-story, 15-25 m high wooden structures averaging 140 m^2 in area, typically separated by streets but 12-18 m wide; 50-67% of the surface was structure-covered.[#] Surrounding this core (which dated to medieval times) were wood and masonry buildings of three-to-six stories, dating from the eighteenth century. More specifically, the residential Hammerbrook section (where the firestorm occurred) was characterized by four-to-five-story houses, with wooden beam ceilings and wooden roofs, erected from 1878-1895 (Schubert 1969). Despite precautions, there was some storage of inflammable fuels within some thin-walled structures.

The average July temperature is 290 K, and July has the highest precipitation (8.9 cm), on a climatological basis. But in the three weeks prior to the raids in late July, precipitation was 4.44 cm, the largest amount falling in thunderstorms on 22 July (Ebert 1963). Even this

---

[#]Comparable figures for "built-upness" in the United States is about 40% for industrial and commercial areas, with approximately 10-25% being typical for residential areas. In the firestorm-destroyed section of Hamburg, there was estimated to be up to 157 kg of wood/m^2, whereas in Japanese cities typical fuel loading was 24 kg of fuel/m^2 (Defense Civil Preparedness Agency 1973); California cities have been estimated (Rodden et al 1965) to have 22-24.5 kg of fuel/m^2. (A typical heating value is 1.86×10^4 kJ/kg for the fuel available.)

moisture was offset by extremely high temperatures that dried out the timber of structures; peak daily temperatures were 294-300 K between 15 July and 25 July. While relative humidities were unusually high early in the month (78% was the lowest reading at 7 a.m., 56% the lowest at 9 p.m., from 1 July to 24 July), the relative humidity remained unusually low thereafter [median humidity of 40% (Schubert 1969)], and skies were clear from 24-28 July. On 27 July, the day before the firestorm-inducing raid, the afternoon relative humidity remained under 30%; the peak temperature reached 305 K at the meteorological station (10 km north of the firestorm section) on both 27 July and 28 July (Bond, ed. 1945), and the temperature at the city center is estimated to have been 308-312 K.

Bombing raids of 24-25 July left a blanket of smoke and haze over the city, a blanket which absorbed excessive amounts of solar insolation by day and which prevented normal heat loss from the surface by night. The stratum of warm air persisted during the early morning hours of 27 July and created a strong temperature inversion to 390 m at 0500 GMT. Cool air was then introduced aloft, as a weak occluded low-pressure system passed to the north of Hamburg. The near-surface lapse rate in the evening was nearly dry adiabatic (Long 1967); i.e., there was a condition close to mechanical instability.[#] The wind at ground level on 27 July was calm to 3.6 m/s generally from the east-southeast. Ebert (1963) quotes eyewitness reports that 20 min before midnight (at the time the raid began) there was no wind, though discerning light wind from no wind at night seems a subtle distinction.

At 12:33 a.m. on 27 July 1943, 750 four-engine Halifaxes and Lancasters of the Royal Air Force Bomber Command dropped 2.17×10^6 kg of high explosives, land mines, and incendiaries on Hamburg; at 2:40 p.m. on 25 July, with the fires still raging from the initial assault, a second air raid involving (inter alia) 218 Flying Fortresses of the 8th Bomber Command of the U.S. Army Air Force continued the raid. At 10:38 a.m. on 26 July, 54 Flying Fortresses bombed Hamburg, and about nine twin-engine Mosquito

[#]At the Hamburg airport at 1700 GMT on the evening of 27 July the temperature fell from 303 K at ground level to 295 K at 510 m, and fell 0.87 K/100 m between 300 and 3750 m. At 3050 m the temperature was 275 K, whereas by the dry-adiabatic lapse rate (1 K/100 m) it would have been 273 K.

bombers added a few bombs on 27 July. At 11:40 p.m. on 27 July, 739 heavy British bombers dropped 2.19 x 10^6 kg of incendiaries and high-explosive bombs on the eastern and southeastern (residential) districts of Hamburg. On 29-30 July, 726 Halifaxes and Lancasters dropped still another 2.16 x 10^6 kg of incendiaries and high-explosive bombs on Hamburg. Commencing at 1 a.m. on 3 August, in a stormy-weather-hampered raid, Lancasters added 1.29 x 10^6 kg of incendiaries and high-explosive bombs on Hamburg. Details are given by Caidin (1960) and by Miller (1968). Despite comparable target, weather, bomb load, and bomb type, of all these raids, only the saturation bombing begun at 11:40 p.m. on 27 July produced a firestorm; thus, developing predictive capability seems a challenging task.

In the firestorm, perhaps 1500 ignitions (Caidin 1960) produced fires that merged into one massive holocaust on the time scale of one-half hour to one hour (estimates vary). In an area of more than 16 km^2, two of every three buildings were simultaneously on fire, and a sea of fire characterized a central area of 3.1 km^2. The fire continued to intensify for 2-3 hours, and 25-30-year-old trees were uprooted (Miller 1943) by radially inward surface winds, which reached 13-18 m/s near the center of the firestorm (with peak estimates in narrower streets of 50 m/s); however, on the outer perimeter very distinct counterclockwise (i.e., cyclonic) tangential winds were reported by eyewitnesses in diverse locales (Caidin 1960, p. 86; Ebert 1963, p. 73, 75)[#]. Aircraft at 4500 m were severely buffeted by the updraft, and a cumulonimbus cloud (with typical anvil head) reached 12,000 m. The winds decreased to light and variable after six hours (Ebert 1963), though the fires were not extinguished until after ten hours (Rodden et al 1965).

[#]At 8.4 km from the center the near-surface winds increased from 5 to 15 m/s during intensification. Ebert (1963, p. 75) states that "... the Hamburg fire storm [had] distinct cyclonic vortex structure."

2.3 Dresden

A strong breeze was blowing across Dresden from the southwest and strato-cumulus clouds were drifting across the whole of Central Europe, with electric storms and ice formation, on the evening of 13 February 1945. However, weather conditions permitted execution of saturation bombing over a quarter circle of 2400 m radius in the densely built-up "Old City" sector, where structures (some 1000 years old, with heavy wooden beams and no steel) were splintered and set ablaze; 244 four-engine British Lancasters carried out this first attack from 10:09-10:35 p.m. with 1800-3600 kg high-explosive bombs. A second British 25-min raid commenced at about 1:30 a.m. on 14 February; 650,000 1.8-kg magnesium-thermite bombs were dropped on the target; in this raid, incendiaries constituted 75% of the bomb load. The city appeared a bright sea of violent fire visible to the approaching second armada of 529 Lancasters from 80 km away, and 100 km^2 were ablaze by the time the second-attack group departed. From 12:12-12:23 p.m. on 14 February, Flying Fortresses and Liberators of the U.S. 8th Air Force again bombed the city (7×10^5 kg), and 37 P-51 aircraft strafed targets of opportunity. Fires burned for seven days and seven nights, with sooty ash showering downwind as much as 30 km; 75% of a 29 km^2 area was destroyed.

The firestorm event began 45 min after the initial raid, and reached its peak at the time of the second raid about three hours later. Survivors described hurricane-force winds uprooting and snapping in half giant trees, jets of flame 12-15 m in length sweeping the streets, sounds similar to those of a thundering waterfall or a howling tornado, and roof gables and furnature being blown toward the center of the burning inner city (Irving 1945). Brode (1980) reports that the fire plume reached 10 km. Some heavy cloud bursts brought rain to portions of the city that night (Caidin 1960)[#]. By dawn, with the wind still blowing strongly but now from the northwest, a 5 km high column of yellow-brown smoke, filled with flotsam lifted by the tornadic winds, was visible (Irving 1945). Bricks and tiles were later

[#]Broido (1960) comments that, for incendiary raids with conventional weapons in World War II, damage averaged only 20% less under raining conditions than that produced under "favorable" weather conditions.

found to have been incinerated in the firestorm area [which may have involved 21 km^2 (Rodden et al 1965)], and pots and pans, melted.

Dresden was in the midst of winter, with snow cover. However, large stocks of coal hoarded in cellars ignited to abet the fire; in fact, some cellars remained too hot to enter for weeks. Also, interiors were dry from heating in winter, so the danger of interior ignitions was enhanced.

Dresden does seem to represent an example in which atmospheric stability, rather than the values of the temperature and humidity in and of themselves, is of significance to firestorm genesis. Dresden also seems to be a counterexample to the oft-stated firestorm prerequisite of nil ambient wind.

2.4 Incendiary Raids on Japanese Cities by Conventional Weapons

The roof-space area in densely populated Japanese cities in 1945 was typically 40-50% of the total area, whereas American residential areas are typically 10% built-up. The light, closely spaced construction was of wood, bamboo, and plaster, and highly vulnerable to incendiary bombing. Furthermore, available firefighting equipment and personnel were easily overwhelmed. Also, the B-29, used in bombing of Japanese cities, had superiority in speed, firepower, and ceiling relative to the B-17 and B-24 used in Europe.

In all, sixty-five Japanese cities were bombed, and forty percent of the housing in these cities was destroyed. However, especially pertinent are sixteen massive incendiary raids between 9-10 March 1945 and 15 June 1945, with Tokyo, Nagoya, Osaka, Kobe, and Yokohama being the targets. In these raids, typically about 300 B-29's would reach the target, each carrying 5.4×10^3 kg of bombs (7.26×10^3 kg for low-altitude flights); the raids lasted three hours at first, but eventually were executed in just over two hours. The objective in general was to drop 2.3×10^4 kg of incendiary bombs on each 2.5 km^2 of target, by emitting 227 kg clusters of 2.7 kg oil incendiary bombs at 17 m intervals.[#] On average, 7.2 km^2 would be burned out by the attack (Craven and Cate, eds. 1953).

What is noteworthy from the present viewpoint is that not one fire-storm occurred as a consequence of any of these raids.

Incidentally, the first of the massive raids, in which 334 B-29's were sent with 1.8×10^6 kg of napalm bombs, targeted for a 20-30 km^2, heavily built-up area of northeast Tokyo on 9-10 March 1945, is an often-cited example of a catastrophic wind-aided flame spread. Although the ambient wind was but 2 m/s at the time of the midnight-till-3:30 a.m. bombing, the wind intensified to 14 m/s, and in the next six hours 39.5 km^2 [and one-quarter of the (easily kindled wood-bamboo-plaster) buildings of Tokyo] were burned out, until large firebreaks (e.g., a river) terminated

[#]Other incendiary bombs employed on Japan included a 32-kg napalm bomb and a cluster of about 110 1.8 kg magnesium-thermite bombs. The oil bomb was used against light construction and the magnesium-thermite bomb, against heavy industry (Craven and Cate, eds. 1953).

the spread (Bond, ed. 1946; Craven and Cate, eds. 1953; Thomas and Witts 1977). It is to be emphasized that this propagating conflagration was not a firestorm.

2.5 Hiroshima and Nagasaki

Hiroshima is a flat Honshu seacoast city (aside from one kidney-shaped hill, 74 m high and 0.8 km long on the east side); it is a circularly-shaped city surrounded by hills and peaks. Hiroshima consists of 82 km^2, of which 17 km^2 were densely built up in 1945. Construction covered about 30% of the central 10 km^2 of the city; while there were some reinforced concrete structures, 90% of the construction (Thomas and Witts 1977) was largely wooden, with light frames and hard-burnt black-tile roofs. Half the structures were one story, and half were one-and-a-half-to-two stories. Dwellings were clustered in large groups with no masonry separating walls (Bond, ed. 1946).

At 8 a.m. on 6 August 1945 Hiroshima was experiencing a warm sunny humid summer day: relative humidity was 80%, pressure was 101.8 kPa, and temperature was 300 K (Committee for the Compilation... 1981). There was 16-24 km visibility, few high-altitude clouds, and no rain had fallen for 27 days. In the north of the city there was a northerly wind; in the south of the city a southerly wind -- about one-or-two m/s. At 8:17 a.m. a 1.8×10^7 kg-TNT-equivalent atomic (uranium) bomb exploded at 670± 70 m altitude, 500 m northwest of the city center, about 1 km to the south of the meeting of the winds.

About 13 km^2 experienced serious structural damage and of this, 12 km^2 was totally burned in what is generally described as a firestorm. Hundreds of small fires began merging about one-half hour after bomb explosion[#], a tornadic whirlwind (with inflow, reaching 18 m/s from all directions) arose two-to-three hours later (around 11 a.m.) and persisted roughly four hours (till 3 p.m.), with winds returning to calm near 5 p.m. (Hill 1961). Some smoldering continued for three-to-four days. At the peak of the fire, stone walls, steel doors, and asphalt pavement were described as glowing red-hot.

[#]Lifton (1967), in a remark reminiscent of the explanation for the multiple ignitions following the noontime Great Kanto Earthquake of 1926, attributes many fire starts to overturning of hibachis still lit from breakfast. However, other ignitions were owing to the radiative precursor, which started many fires up to 1.5 km from the Aioi Bridge target (Thomas and Witts 1977), and a few fires up to 3 km away (Committee for the Compilation... 1981).

At 11:02 a.m. on 9 August 1945, a 1.8×10^7 kg-TNT-equivalent atomic (plutonium) bomb was detonated at about 575 m altitude over the Kyushu seacoast city of Nagasaki, about 2 km north of the city center. The weather was bright and clear, with unlimited visibility; it had been ten days since the last rain. The temperature was 302 K, the humidity was 71%, the wind was 3 m/s from the southwest, and the pressure was 101.4 kPa. In these respects, Nagasaki was similar to Hiroshima. However, Nagasaki had a densely built-up area of only 9.5 km^2, though with much the same construction as in Hiroshima except for a larger fraction of industrial buildings. More importantly, Nagasaki consists of coastal strips along both sides of a bay and two long narrow (8 km x 2 km) river valleys separated by a hill 200 m-300 m high. No firestorm occurred at Nagasaki; rather, the southwest wind increased to 18 m/s after the conflagration had become established (perhaps two hours after the explosion) and tended to carry the fire up one valley in a direction in which there was nothing to burn. There was fire spread southward toward the built-up area, but this spread was against the wind and hence slow. A series of small tributaries and canals also served as firebreaks. Seven-to-nine hours later the wind came from the west at about 6 m/s. Thus, owing to different terrain and structural distribution, Nagasaki experienced a progressive, wind-aided fire spread that came under control in 19 hours and was extinguished in about 56 hours after consuming about 2.25 km^2 (Hill 1961).

2.6 Korea and Vietnam

Although up to one-hundred U.S.A.F. B-29's were operational at one time during the Korean War, primarily high-explosive bombs were used on industrial targets; the light-bomber force (B-26's) did drop incendiary bombs on towns, but the built-up area of such targets was generally less than 0.6 km^2. Two reported incendiary attacks against urban areas (Futrell et al 1961) are as follows: (1) about 60% of a 5-km^2 built-up area burned in the aftermath of a noontime raid by 70 B-29's on Sinuiju near the Yalu River on 8 November 1950 (involving 5.31×10^5 kg of 227-kg incendiary clusters); (2) 3.5% of the built-up area of the snow-covered North Korean capital of Pyongyang burned owing to incendiary raids by 63 B-29's on 3 January 1951 and by 60 B-29's on 5 January in 1951. Neither event has been classified as a firestorm. Later incendiary raids were comparable in scale to those on Japanese and Germany cities of World War II [e.g., during an eleven-hour period on 11 July 1952, 1254 aircraft dropped 1.27×10^6 kg of bombs and 88 m^3 of napalm on Pyongyang (SIPRI 1975)]; again, no firestorms ensued.

B-52 bombers, jets, land-based artillery, and naval bombardment were used in a coordinated attempt (via napalm and white phosphorus) to initiate a major fire event in the U Minh Forest in the Delta region of South Vietnam in the spring of 1968, and while burning continued for six weeks, no fire-storm event occurred (SIPRI 1975). Earlier attempts at large-fire creation near Saigon in 1965-1966, and northeast of Saigon in January-April 1967 with magnesuim-thermite incendiary bombs, and later attempts in west central Kontum province in the spring of 1971, were even less successful (Shapley 1972); there is indication that on some occasions fire-engendered rainstorms helped to extinguish the burning [a phenomenon familiar in connection with fire in Hawaiian sugar-cane fields (Morton 1957)[#]]. Tropical rainforests in Vietnam are characterized by prevailing relative humidity of 80%; also, dead vegetation decays so rapidly that there is little ground litter, and chemical defoliants were used in preliminary steps to create combustible fuel.

[#]Dust-and-ash-laden heavy rain ("black rain") followed about a half hour after explosion in both the Nagasaki and Hiroshima areas (Committee for the Compilation... 1979).

These more recent unsuccessful attempts at firestorm generation are cited as further suggestion that the event is rare, dependent on environmental conditions and fuel-loading, and apparently still not fully understood by military specialists.

3. A MODEL OF THE FIRESTORM

3.1 Choice of an Approach

Attention is now turned toward exploring quantitative analysis of (1) the criterion for onset, (2) possible quasi-steady mature-stage structure and (3) the nature of the decay, of a firestorm.

One approach might be to formulate a boundary/initial-value problem, uniformly valid in space and time, encompassing all pertinent thermohydrodynamic phenomena, and then to undertake numerical solution of a finite-difference approximation to the partial differential equations (subject to starting and boundary constraints) on a high-speed digital computer. Among the reasons such an approach is not undertaken here are that formulation of unsteady (turbulent) transfer of mass, momentum, and energy in a buoyant, reacting flow entails parameterization of moot validity; finite-differencing introduces spurious diffusion; lateral and "ceiling" constraints, in view of finite computer storage and speed, may be artifical and vitiate results within the flow domain; and knowledge of initial condition and subsequent behavior is so gross that opportunity for validation by refined comparison with physical data is extremely limited. A far less detailed description may be capable of more directly and economically yielding desired information.

Accordingly, a roughcut model of the firestorm is now very briefly set forth to motivate the analyses undertaken below. The firestorm is subdivided into three or four domains, in each of which different physical processes are of dominant importance in the balances for conservation of mass, momentum, and energy; enforcement of appropriate requirements for continuity of thermodynamic and dynamic quantities and their fluxes at the interfaces between domains ensures that the locally valid descriptions combine to constitute a self-consistent global description, taken to be unique. The trial subdivisional analysis proposed for firestorms continues the analogy (introduced earlier) with severe vortical convective (meteorological) storms of the troposphere, since the subdomains are very closely related to those found useful in examining a variety of rapidly rotating atmospheric flows ranging in lateral scale from the tornado to the tropical cyclone (Barcilon 1967; Carrier, Hammond, and George 1971; Carrier 1971a, 1971b;

Fendell 1974; Carrier and Fendell 1978). The model combines entirely conventional, long-established features with some more novel proposals.

3.2 The Mature-Stage Structure -- Overview

It seems convenient to begin with a model of the (tentatively postulated) quasi-steady, fully developed, very intense firestorm. Tracing its antecedents and dissolution becomes more and more challenging as one moves toward earlier and later events because it becomes less and less valid to separate off a readily definable volume of the atmosphere and to concentrate entirely on processes occurring within that volume. At far earlier and far later times, transfer across the boundaries of the volume become important. Furthermore, identification of a few dominant processes is less readily done as one approaches smaller perturbations about typical meteorological conditions.

The volume of interest extends vertically from ground level to the level of neutral stability (defined below), and laterally from the axis of rotation (taken as vertical) to where the rotation is essentially reduced to negligible level (say, one-or-two percent of its peak value). It is taken that there is negligible convective transport across the boundaries of this volume, though there may be diffusive transport across the boundaries. Within the volume, an axisymmetric description is taken to hold. The thermodynamic state as a function of altitude is taken to be known, to any degree of accuracy required, at the lateral edge of the volume. At the top of the volume is an isothermal, isobaric slippery "lid", such that air can move laterally, but not vertically. The radially invariant temperature and pressure and relative humidity (the last probably being zero, to excellent approximation) at the altitude of the lid may be taken to be those of the ambient air at the same altitude.

Because the air in the volume is rotating, from conservation of radial momentum the pressure at the center of the volume is reduced from the pressure at the outer edge, at the same altitude. The rotational motion is implicitly reduced at the altitude of the lid, relative to its value at lower altitude; in fact, the ambient angular momentum may be stratified, where "ambient" here and henceforth is a brief expression for "pertaining to the lateral boundary". From hydrostatics, which is an adequate approximation over the height of the volume for immediate purposes, for such a pressure deficit to hold, the weight of a vertical column of air near the center of the volume is less than the weight of an ambient vertical column,

i.e., the density tends to be lower near the center of the volume. In the present context, the central density is lower because the air there has been heated by intensely exothermic chemical reaction. If one takes as known the enthalpy increase per unit mass of central gas as a function of altitude, then one can compute how the temperature and density (of originally ground-level ambient air) vary as a function of pressure, under the assumption of adiabatic ascent; i.e., for definition of the lid, ascent is idealized as so rapid that no entrainment of cooler air occurs during ascent, and only expansional cooling occurs. The lid lies where the pressure and temperature of such an adiabat matches the temperature and pressure of the ambient, and the altitude assigned to this lid is the ambient height. By use of hydrostatics, one can now assign an altitude to each thermodynamic state along the adiabat by beginning with the lid pressure, assigned at lid height; the pressure assigned at ground level gives the pressure differential available to sustain swirling by cyclostrophic considerations (if one neglects frictional effects very near the ground arising from enforcement of the no-slip boundary condition). If one adopts radial profiles for density and for the azimuthal component of velocity (e.g., say for convenience, radially invariant density and a Rankine-vortex profile for the swirl, with neither the magnitude nor the site of the peak swirl assigned), then from cyclostrophy one obtains the peak swirl consistent with the ground-level radial pressure differential.[#]

This calculation probably yields the peak swirl attained anywhere in the firestorm.[†] But is it the highest conceivable value consistent with plausible, if idealized, atmospheric processes? The answer is no, if one argues by analogy with severe convective stor s. It is observed that tropical cyclones can undergo a transition from a tropical storm to a more intense stage referred to as a hurricane or typhoon. In this transition, a compressionally heated slow downdrift of originally near-neutral-stability-level, dry, virtually nonrotating air descends along the axis of rotation, and the swirling convective motion then occurs in an annular domain

[#]It is convenient to approximate the lateral boundary as infinitely far distant from the axis of rotation in this calculation.

[†]For completeness, there may be a modestly higher value achieved in a small subdomain referred to as the "turnaround" (see below).

displaced from the axis of rotation; an "eye" has been inserted within an "eyewall". The compressional heating of the slow central recirculation is such that the radial pressure deficit (from ambient value) at the bottom of the atmosphere is greater in the presence of an eye than in the absence of an eye. Actually, the eye/eyewall interface slopes radially away from the axis of rotation with increasing height, so that a vertical column of air exists whose base is in the eyewall and whose top is in the eye. Thus, meteorologically, hydrostatic and cyclostrophic considerations combine to yield a much higher peak swirl value in the presence of a well-developed eye (say, 100 m/s) than in the absence of an eye (say, 50 m/s).[#] However, whereas crudely half of all tropical storms intensify to become typhoons or hurricanes, cited wind-speed levels in firestorms suggest that possibly no significant eye formation occurs. (Admittedly the peak levels cited in firestorms concern low-level radially inward wind, but it is explained below that the peak radial winds near ground level are comparable in magnitude to the peak swirl speed, which occurs at a somewhat higher altitude.) Nevertheless, smoke, dust, and debris obscure the nature of the core flow at altitude in a firestorm, and for a "worst-case" calculation the possibility of eye insertion should be considered.[§] Indeed, observations of intense Australian bushfires indicate several occasions, at peak burning, of clouds above the top of the convection column clearly being drawn down into the column (Taylor et al 1973).

[#]The higher peak swirl value with an eye is a result not only of greater low-altitude radial pressure deficit from ambient, but also of the fact that none of the deficit is "expended" to maintain eye rotation (the eye is virtually nonrotating). Without an eye, the pressure deficit from ambient is less and about half is expended to maintain near-rigid-body rotation of the near-axis air in a Rankine vortex.

[§]Even in typhoons, eye insertion is usually incomplete, in that the eye is not entirely dry and does not extend the entire distance from the neutral-stability altitude to sea level. Furthermore, eye insertion may be transitory, in that transition back and forth between one-cell structure (no eye) and two-cell structure (with an eye) is common.

3.3 The Mature-Stage Structure -- Refinements

The subdivisions of the adopted model for the mature-stage structure are (1) the bulk vortex; (2) the surface inflow layer; (3) the turnaround and convective column; and, sometimes, (4) the eye. Clearly, earlier reference (Section 3.1) to a three-or-four-part structure alluded to the fact that an eye may or may not be present. It is reiterated that the subdivisions are selected on the basis of distinction of dominant physical processes; the sizes of the subdomains vary enormously.

In the bulk vortex, which constitutes most of the volume, there is a cyclostrophic balance radially (radial pressure gradient inward balancing centrifugal acceleration outward), so that there is very modest radially inward motion (only enough to keep the central convective column from drifting radially outward). The principal velocity component is the swirl, which decreases roughly inversely with distance from the axis, the peak swirl occurring at the point of this subdomain closest to the axis of rotation, the radial pressure gradient varies compatibly. There is a broad slow downdrift in the bulk (potential) vortex. The thermodynamic stratification at all radial positions is roughly that of the ambient at altitude; the enthalpy is augmented at low altitudes owing to the fire.

In the surface inflow layer, the only subdivision in which angular momentum is not conserved, the cyclostrophic balance is upset because whereas the radial pressure gradient holds unaltered across this thin surface layer, the no-slip boundary condition alters the centrifugal acceleration. The result is that there is swirling radial inflow, supplied by the broad slow downdrift from the bulk vortex above. The surface inflow layer monotonically increases in thickness with decreasing radial distance from the axis of rotation (and of symmetry), owing to augmented throughput; it has almost zero thickness in the ambient and perhaps grows to, very crudely, 20-40 m, in thickness, though its rate of growth is relatively small as the center of the vortex is approached. Because there is an accelerating pressure gradient above this near-ground-boundary layer, the role of frictional retardation enforcing the no-slip boundary condition becomes confined to a thin (and thinning) ground-contiguous sublayer of the surface inflow layer; thus, as one approaches the axis of rotation (i.e., under the high-speed portion of the bulk

vortex), there is no retardation of the motion except very near the ground. At fixed radial distance from the axis of rotation, as one descends axially from the bulk vortex across the thickness of the surface inflow layer toward the ground, the wind speed remains unaltered in magnitude until one gets exceedingly close to the ground (i.e., until one reaches the very thin ground-contiguous sublayer); while the magnitude of the wind remains invariant, the direction of the wind changes from pure swirl (with negligible radial inflow) to pure radial inflow (with negligible swirl). This point is noteworthy because one infers, from observation of intense radially inflow near the surface, the existence of intense swirling flow above. Further from the axis of rotation, i.e., at large radial positions, swirling inflow of reduced magnitude is noted, since friction acts across the thickness of the entire surface inflow layer, and no such complete "tradeoff" of swirl for inflow occurs. [This description should be compared with reports from eyewitnesses of the Hamburg firestorm presented by Ebert (1963).] The swirling inflow of the surface layer necessarily becomes a swirling updraft close to the axis of rotation. Because the mass rising in the central convective column is furnished almost entirely through its near-ground base in a rapidly rotating environment, that surface-level throughput must be large, and hence large surface winds seem reasonable.[#]

Geometrically, then, one sees that the broad slow downdrift into the surface inflow layer is conveyed upward in a central region of modest cross-section; hence an appreciable axial velocity component in the convective column is to be expected from continuity. Since conservation of angular momentum holds for most of the column, appreciable swirl is also to be expected in the convective column. In the low-altitude turnaround region, in which the swirling inflow layer becomes the swirling upflux of the convective column, those streamlines closer to the ground approach closer to the axis of rotation; but streamlines closer to the ground have

[#]Smith et al (1975) acknowledge the existence for stationary large fires of a "concentrated inflow", a "... relatively shallow inflow over the fire perimeter known as the fire wind." Numerical solution is given for buoyant viscous flow, induced by a centrally sited finite hot plate in the ground plane, for a two-dimensional, Cartesian geometry (such that angular-momentum considerations do not enter). An appreciable inflow confined to a near-ground layer does not arise in the computed results.

entered the inflow layer at larger radial distance from the axis of rotation, where friction is still active across the inflow layer, so such streamlines convey less angular momentum than streamlines that enter the inflow layer at smaller radial distance from the axis of rotation. Hence, it is possible that swirl speeds modestly in excess of the peak swirl of the radially-inward-most position of the bulk vortex is achieved. As the convective column rises high into the volume, decrease of density with altitude suggests, from conservation of mass, that the column broadens in cross-section, and, from conservation of angular momentum, that the swirl speed decreases. As the density discrepancy between the fire-heated air of the convective column and surrounding bulk-vortex air decreases, the buoyant acceleration decreases and the column spreads over the top of the bulk vortex in a broad, slow radially-outward-moving layer near the lid. The decrease of density discrepancy occurs slowly with altitude, so the convective column extends to exceptional altitude, in a rotating environment; as already hinted, mixing of convective-column air with turbulently entrained, cooler, heavier surrounding air is greatly reduced if the surrounding air is appreciably rotating, because the cyclostrophic balance of pressure gradient and centrifugal acceleration in the surrounding vortex inhibits such entrainment.[#] Ying (1965) has quantitatively inferred the very significant reduction of entrainment into a convective column as a function of the angular momentum of the surrounding rotating air in a laboratory apparatus simulating a firewhirl[†]. With access to oxygen limited by reduced entrainment, burning of pyrolyzed fuel vapor rising in the convective column may continue to exceptional height. Thus, the unusual altitudes to which flame is observed and to which the convective column is observed to rise in a firestorm seem consistent with this model.

[#]This mechanism is presented rather artificially by Ebert (1963) in an otherwise excellent presentation, and cogently by Michaud (1975) in an otherwise moot proposal.

[†]The significance of this appreciable reduction of entrainment of surrounding air into the convective column, such that a persistent density discrepancy permits ascent high into the troposphere, may be emphasized by noting that the magnitude of the entrainment constant introduced by Morton, Taylor, and Turner (1956) had proven to be surprisingly invariant to all parametric changes prior to consideration of rotation.

As already noted, insertion of a compressionally heated nonrotating downdrift near the axis of symmetry, such that the convective column becomes an annulus displaced from the axis, is possible, at least for a range of altitudes extending a small distance downward from the lid. The air in the "eye" may have been entrained out of the convective column, since the air at the inner edge (i.e., near-axis portion) of the convective column may well be rotating least and mixing fastest, at least at lower and midtropospheric altitudes: this is the distribution that exits from the surface inflow layer, and only a lower-tropospheric "vortex breakdown" in the convective column is likely to alter it appreciably. Thus, the air in the eye is slowly recirculating, drifting downward near the axis and, away from the axis, sheared upward by the convective-column motion. Precisely why an eye (nascent or extensive) becomes inserted in some atmospheric vortices and not in others seems unresolved. Two conjectures are (1) the stratification of the ambient angular momentum is significant, and/or (2) residual effects of the nature of the transient spin-up, by which the mature-stage structure described here is achieved, are significant.

3.4 Spin-Up and Decay

Simplistic competition between convectively induced advection and radial (turbulent) relaxation seems an incomplete description of how the above system forms or decays, except very early or very late in the life cycle (Dergarabedian and Fendell 1967).

The "flushing" of the original air out of the central column and its replacement by lighter high-enthalpy air[#] in a system in which organized rotation is already discernable has been described in roughcut fashion (Carrier 1971b); this work probably pertains mainly to the final stages of spin-up. However, this work does describe how the surface inflow layer enters into consideration early in the life cycle, and how radial influx (negligible in the bulk vortex in a strongly rotating system) is appreciable through the depth of the volume during spin-up and is only gradually suppressed. Thus, one can expect appreciable entrainment (probably in the form of gulping-type entrapment of surrounding air taken deep into convective column) prior to spin-up. This work also suggests that, as fluid particles of the developing bulk vortex move closer to the axis of rotation[†], to an extent consistent with the radial pressure gradient engendered by flushing the convective column of original ambient air and replacing that air with higher-enthalpy air, the particles overshoot their equilibrium position. The result is an inertial oscillation (possibly slowly damped), in which the convective column periodically expands and contracts; during successive rarefactions of the core, perhaps an intermittent or a gradually-better-defined eye could be inserted. However,

---

[#]The enthalpy here implicitly refers to the total static enthalpy, the sum of the sensible heat, the gravitational potential energy, the latent heat that could be released by a water vapor present, and another source present (as heat of chemical reaction). The dynamic contribution in highly subsonic atmospheric flows is usually regarded as relatively negligible, even for very severe vortical storms. If one takes all the chemical heat as introduced at the base of the convective column, then the total static enthalpy is invariant with altitude for a convective column in the absence of mixing.

[†]If spin-up entails particles (possessing finite angular momentum in the ambient) moving closer to the axis of rotation, then a swirl velocity component that decays inversely with radial distance from the axis of rotation is plausible.

more refinement of the structural details of the core flushing are required, since roughhewn lifting is probably inadequate as a description of the convective-column flushing.

It seems pertinent to cite documentation of firewhirls [e.g., Lochneiss 1966; Pirsko et al 1965] which persist as vigorous vortices for several minutes after translating out of the fire which spawned them. In such cases, in terms of the present model, the contents of the inflow surface layer and the contents of the bulk vortex must continue to furnish a high-enthalpy throughput supply for the system; in the sense that the cyclostrophic balance renders the air mass of the bulk vortex "captured", this persistence of the vortex seems possible. However, it does suggest that radiative transfer, and possibly local plume action countering the broad slow downdrift, does augment above the ambient level the enthalpy of an appreciable amount of lower-tropospheric air of the bulk vortex.

This discussion of the trial model of the firestorm is concluded with an important qualification that deserves especial attention. While, for purposes of an overview and for ease of exposition, it seemed worthwhile to dwell on the mature-stage, quasisteady structure of a fully developed intense convective vortex (Sections 3.2 and 3.3), and while, for completeness, it seemed worthwhile to note that some short-lived fire-associated vortices seem to attain properties attributable to the fully developed vortex (previous paragraph), severe firestorms do <u>not</u> persist for more than a <u>few hours</u> before the fuel supply (combustible matter) is exhausted. There are two significant implications. First, there is <u>not</u> time for air to be drawn in from large radial distances in a firestorm, and hence there is <u>not</u> time for spin-up to very large speeds. In contrast, a typhoon may involve intensification over the <u>temporal span of weeks</u>, with air drawn inward from well over 1000 km to attain speeds sometimes over 100 m/s. Also, after the long summer heating, there is copious water vapor in the atmosphere over vast expanses of tropical ocean to supply the typhoon. But only limited portions of a city are likely to have the combustible-fuel loading to sustain a firestorm for more than six hours, the same time scale associated at midlatitudes with the component of the rotation of the earth perpendicular to the surface. While the radial inrush through narrow city canyons may attain 25 m/s on very unusual occasions, there is no firm

reason to expect spin-up to swirl speeds approaching this magnitude. Second, with the fairly abrupt exhaustion of fuel, a firestorm may be expected to proceed from the intensification stage to the decay stage without ever attaining quasisteady mature-stage structure. Thus, for example, while rotation may reduce entrainment over much of the troposphere, it may well be that the influx to the plume is not entirely confined virtually to a near-ground layer. Hence, it is appropriate that time-dependent treatment of firestorm spin-up be undertaken as the practically important problem (next section).

4. CRITERIA AND TIME SCALE FOR THE ONSET OF A FIRESTORM

4.1 Introduction

The point of view taken is that a fully-established convective column exists over a maintained heat source of known strength (total enthalpy released per unit time) in an atmosphere of known stratification (temperature and relative humidity as a function of pressure). That is, a now-classical entraining, nonrotating plume exists above a fire, which is (tentatively) approximated as a point source of heat, without associated release of momentum per unit time or mass per unit time. In this way, but one overall parameter characterizes the fire, and probably unavailable detail is not required.[#] A conventional integral-type plume theory yields the vertical structure of this convective column, in particular, the width, upward speed, and density discrepancy from ambient as a function of altitude above the source. Typically, the plume spreads as the speed of ascent slows, ultimately to zero, owing to entrainment of heavier surrounding air into the convective column. This known solution serves as an initial condition to the questions of interest here: as a function of the heat-source strength, ambient stratification, and ambient circulation, how long would spin-up require and how is the structure of the convective column altered?

These questions require three innovations. The aspect of time development must be added to description of flow over a maintained source (as opposed to time dependence associated with the starting plume or buoyant thermal). Also, conservation of angular momentum enters, and conservation of radial momentum must be retained since existence of appreciable swirl implies existence of a significant radial pressure gradient (as opposed to a statement of radially invariant pressure, to which the conservation of radial momentum degenerates for a nonrotating column). Finally, the effective reduction of the entrainment parameter with spin-up of the ambient must be quantified.

[#]Typically all that is available to characterize a site under study is its area, the fuel loading (average mass of combustible matter per unit area), and the exothermicity (heat released per unit mass of combustible matter, with adjustment, if required, for drying prior to burning).

Two other innovations are not considered. The first includes provision for two-cell structure, i.e., for downdrift, at least near the axis within an annular upflux at the top of the column. The second includes provision for mass and momentum influx into the base of the convective column from the surface inflow layer formed on an effectively nonrotating ground plane under a rapidly rotating vortex. With the omission of these considerations, the model being developed seems adequate only for early stages of spin-up.

4.2 Formulation

Attention is now turned to an axisymmetric treatment in cylindrical polar coordinates (r,Θ,z), with corresponding velocity components (u,v,w), of a plume above a maintained point source of strength E. Specifically,

$$M \equiv \pi \int_0^{b\to 0} \rho\, w\, r\, dr, \tag{4.2.1}$$

$$\phi \equiv \pi \int_0^{b\to 0} \rho\, w^2\, r\, dr, \tag{4.2.2}^{\#}$$

$$E \equiv \pi \int_0^{b\to 0} \rho\, w\, c_p\, T_a \left(\frac{T - T_a}{T_a}\right) r\, dr, \tag{4.2.3}$$

where the mass source $M = 0$, the momentum source $\phi = 0$, but the enthalpy source E is finite and given. Also, the plume radius $b \to 0$ as $z \to 0$; i.e., the point source is assigned to be at $z = 0$. Here ρ is density, T is temperature, c_p is heat capacity of the gas, and subscript a refers to ambient conditions, i.e., to conditions outside the plume where (in the absence of rotation) thermodynamic quantities are a known function of z only.

The flow is so subsonic that the density, except for the gravitational term in the momentum equation is well approximated by its ambient value, and variance of the temperature from ambient is linearly related to the variances from ambient of pressure and density. However, in distinction to the (conventionally adopted) strict form of the Boussinesq approximation,

---

[#] A point source of both mass and momentum cannot exist (Morton 1959).

the ambient values here are permitted to vary with altitude, a necessary generalization in view of the tropospheric scale of the phenomena under study. It should be emphasized that no provision for axially distributed chemical exothermicity in the portion of the plume under study is included; such burning occurs at lower altitudes during early spin-up, and existing models of burning in turbulent buoyant convection are of uncertain validity.

The conservation equations for mass, radial momentum, axial momentum, and energy are taken to be described adequately by the following relations (subscripts r,z denote partial differentiation):

$$\left(\rho\, r\, w\right)_z + \left(\rho\, r\, u\right)_r = 0; \tag{4.2.4}$$

$$\left(\rho\, r\, u\, w\right)_z + \left(\rho\, r\, u^2\right)_r + r\, p_r - \rho\, v^2 = 0; \tag{4.2.5}$$

$$\left(\rho\, r\, w^2\right)_z + \left(\rho\, r\, u\, w\right)_r + r\, p_z + \rho\, r\, g = 0; \tag{4.2.6}$$

$$\left(\rho\, w\, r\, c_p\, T\right)_z + \left(\rho\, u\, r\, c_p\, T\right)_r + \rho\, r\, g\, w = 0. \tag{4.2.7}$$

Conservation of angular momentum is discussed below. Here p is pressure and g is the magnitude of the gravitational acceleration.

The following Gaussian description is adopted for the dependent variables:

$$w(r,z) = W(z)\exp\left[-r^2/b^2(z)\right], \tag{4.2.8}$$

$$p_a(z) - p(r,z) = \sigma(z)\exp\left[-r^2/b^2(z)\right], \tag{4.2.9}$$

$$g\,\frac{\rho_a(z) - \rho(r,z)}{\rho_a(z)} = f(z)\exp\left[-r^2/b^2(z)\right], \tag{4.2.10}$$

$$r\, v(r,z) = b(z)V(z)\left\{1 - \exp\left[-r^2/b^2(z)\right]\right\}, \tag{4.2.11}$$

where $V(z)$, $W(z)$, $\sigma(z)$ are anticipated to be positive, and $f(z)$ is positive at small z at least.

Additional relations are as follows (R is the gas constant for air):

$$p(r,z) = \rho(r,z)R\,T(r,z) \Longrightarrow p_a(z) = \rho_a(z)R\,T_a(z); \qquad (4.2.12a)$$

$$\frac{T(r,z) - T_a(z)}{T_a(z)} \doteq \frac{1}{T_a(z)}\left(\frac{\partial T}{\partial p}\right)_\rho \left[p(r,z) - p_a(z)\right] + \frac{1}{T_a(z)}\left(\frac{\partial T}{\partial \rho}\right)_p \left[\rho(r,z) - \rho_a(z)\right], \qquad (4.2.12b)$$

where $(\partial T/\partial p)_\rho$ and $(\partial T/\partial \rho)_p$ are both evaluated in the ambient. Hence,

$$\frac{T(r,z) - T_a(z)}{T_a(z)} = \frac{p(r,z) - p_a(z)}{p_a(z)} - \frac{\rho(r,z) - \rho_a(z)}{\rho_a(z)}. \qquad (4.2.13)$$

Again, the deviations from ambient air taken as small, in distinction to the modeling of Morton et al (1956), in which the deviations from source level are taken as small. Also the so-called Taylor entrainment parameter α is introduced:

$$-\lim_{r\to\infty}(r\,u) = \alpha\, b(z)W(z), \qquad (4.2.14)$$

where α is a function at most of the variables introduced by swirl, i.e., $V(z)$, $\sigma(z)$. In the absence of swirl α is taken as a universal constant of value $\alpha_0 (\equiv 0.093)$.

Boundary conditions are discussed after the equations are reduced. However, it is remarked that, despite the conveniently abbreviated notation, b, σ, f, W are at least parametrically functions of time t. Consideration of conservation of angular momentum below results in an explicit temporal derivative of V. Thus, for example, it would be more precise to write

$$w(r,z;t) = W(z;t)\exp\left[-r^2/b^2(z;t)\right]; \qquad (4.2.15)$$

however, no confusion should arise from the abbreviated notation.

Integration of (4.2.4) over r from r = 0 to $r \to \infty$ yields, by use of (4.2.8) and by setting $\rho(r,z) \doteq \rho_a(z)$,

$$\frac{d}{dz}\left(\rho_a\, W\, b^2\right) = 2\,\alpha\,\rho_a\, W\, b. \qquad (4.2.16)$$

The first two terms on the left-hand side of (4.2.5) are anticipated to be negligible;[#] the remaining (cyclostrophic) balance is

---

[#]It is suggestive that the second term of (4.2.5) as written is a perfect differential vanishing at $r \to 0$, since $r\,u^2 = O(r^3)$ as $r \to 0$, and at $r \to \infty$, since $u(r \to \infty) \to 0$, $(r\,u)u \to (\alpha\, b\, W)u \to 0$. The first term is, upon integration over r,

$$\frac{d}{dz}\left\{W(z)\int_0^\infty \rho\, r\, u\, \exp\left[-r^2/b^2(z)\right]dr\right\},$$

where, from integration of (4.2.4) from r = 0 to general r with $\rho \to \rho_a$,

$$\rho\, r\, u = -\frac{d}{dz}\left[\rho_a\,\frac{b^2\, W}{2}\left\{1 - \exp\left[-r^2/b^2(z)\right]\right\}\right].$$

Hence the second term is

$$-\frac{d}{dz}\left\{\left(\rho_a\, W\,\frac{b^2}{2}\right)_z\, b\, W\int_0^\infty \left[1 - \exp(-x^2)\right]\exp(-x^2)dx\right\}$$

$$+\frac{d}{dz}\left\{\rho_a\, W^2\, b^2\, b_z\int_0^\infty x^2\exp(-2x^2)dx\right\},$$

or, by use of (4.2.16),

$$\frac{d}{dz}\left\{-\frac{2^{\frac{1}{2}}-1}{2}\left(\frac{\pi}{2}\right)^{\frac{1}{2}}\alpha\,\rho_a\, b^2\, W^2 + \frac{1}{8}\left(\frac{\pi}{2}\right)^{\frac{1}{2}}\rho_a\, b^2\, b_z\, W^2\right\}.$$

For $b = O(\alpha\, z)$ with α small, this term is anticipated to be relatively small.

$$\int_0^\infty p_r \, dr = \int_0^\infty \rho \frac{v^2}{r} \, dr. \tag{4.2.17}$$

If $\rho \to \rho_a$, from (4.2.9) and (4.2.11),

$$\sigma = I \rho_a V^2, \tag{4.2.18}$$

where

$$I = \int_0^\infty \frac{[1 - \exp(-x^2)]^2}{x^3} \, dx = \ell n \, 2. \tag{4.2.19}^{\#}$$

In the ambient,

$$(p_a)_z + \rho_a g = 0. \tag{4.2.20}$$

$$I = \int_0^\infty \frac{[1 - \exp(-x^2)]^2}{x^3} \, dx = \frac{1}{2} \int_0^\infty \frac{[1 - \exp(-u)]^2}{u^2} \, du$$

$$= -\frac{1}{2u} \left[1 - \exp(-u)\right]^2 \Big|_0^\infty + \int_0^\infty \frac{1 - \exp(-u)}{u} \exp(-u) du.$$

For $\varepsilon \to 0$,

$$I = \int_0^\varepsilon \frac{1 - \exp(-u)}{u} \exp(-u) du + \int_\varepsilon^\infty \frac{\exp(-u)}{u} \, du - \int_\varepsilon^\infty \frac{\exp(-2u)}{u} \, du$$

$$= \int_\varepsilon^\infty \frac{\exp(-u)}{u} \, du - \int_{2\varepsilon}^\infty \frac{\exp(-u)}{u} \, du = \int_\varepsilon^{2\varepsilon} \frac{\exp(-u)}{u} \, du$$

$$= \ell n \, u \Big|_\varepsilon^{2\varepsilon} = \ell n \, 2.$$

Multiplying this equation by r and subtracting from (4.2.6) yields, upon integration over r and use of (4.2.9),

$$\frac{d}{dz} W^2(z) \int_0^\infty \rho r \exp\left[-\frac{2r^2}{b^2(z)}\right] dz - \frac{d}{dz} \sigma(z) \int_0^\infty r \exp\left[-\frac{r^2}{b^2(z)}\right] dr$$

$$+ \rho_a(z) \int_0^\infty g \frac{\rho - \rho_a(z)}{\rho_a(z)} r \, dr = 0, \tag{4.2.21}$$

since the perfect differential vanishes as $r \to \infty$ because $w \to 0$. Hence, if $\rho \to \rho_a$ in the first term and if use is made of (4.2.10) in the last term,

$$\frac{d}{dz}\left[\left(\frac{\rho_a W^2}{2} - \sigma\right) b^2\right] = \rho_a f b^2. \tag{4.2.22}$$

Equation (4.2.7) may be rewritten

$$\left\{\rho w r\left[c_p\left(T - T_a\right)\right]\right\}_z + \left\{\rho u r\left[c_p\left(T - T_a\right)\right]\right\}_r = -\rho w r c_p T_{a_z} - \rho w r g; \tag{4.2.23}$$

if $\rho \to \rho_a$ on both the left-hand and the right-hand sides, then by use of (4.2.12a), (4.2.20), and the relations $R = (c_p - c_v) = c_v(\gamma - 1)$,

$$\left\{\rho_a w r\left[c_p\left(T - T_a\right)\right]\right\}_z + \left\{\rho_a u r\left[c_p\left(T - T_a\right)\right]\right\}_r$$

$$= -\frac{p_a w r}{\gamma - 1} \frac{d}{dz}\left[\ell n\left(\frac{p_a}{\rho_a^\gamma}\right)\right]. \tag{4.2.24}$$

Integration over r from r = 0 to $r \to \infty$, by use of (4.2.8), (4.2.12a), and (4.2.14), yields

$$\frac{d}{dz}\left[\left(p_a W b^2\right)\left(\frac{f}{g} - \frac{\sigma}{p_a}\right)\right] = -\frac{2}{\gamma}\left(p_a W b^2\right) \frac{d}{dz}\left[\ell n\left(\frac{p_a}{\rho_a^\gamma}\right)\right]. \tag{4.2.25}$$

Attention is now turned to conservation of angular momentum. Let $\tilde{R}$ be the radial distance at which a particle originally lies if that particle enters the plume when the plume dimension is b. Also, let Ω be the normal component of the rotation of the earth (in radians per unit time) at the latitude at which the event occurs. Then, the absolute angular momentum at $\tilde{R}$, which is $\Omega\tilde{R}^2$, equals the angular momentum association with the rotation of the earth at b, which is Ωb^2, plus the angular momentum relative to the earth at b, which from (4.2.11) is approximately bV. Explicitly,

$$bV + \Omega b^2 \doteq \Omega\tilde{R}^2, \tag{4.2.26}$$

where $\Omega b^2 << bV$ for most conditions of interest. That is, the angular momentum at b in noninertial coordinates is, for most conditions of interest, approximately equal to the absolute angular momentum at $\tilde{R}$. In any case, differentiation with respect to time (denoted by a super dot) yields

$$\dot{V}b = 2\Omega\tilde{R}\dot{\tilde{R}}, \tag{4.2.27}$$

since b is taken to change slowly in time relative to $\tilde{R}$ and V. Now $\tilde{R}$ is initially large, and increases in magnitude with time, even though the convection induces influx; i.e., $\dot{\tilde{R}} = -u$ in (4.2.4):

$$\rho_a \tilde{R}\dot{\tilde{R}} = \int_0^{\tilde{R}} \left[\rho_a W r \exp(-r^2/b^2)\right]_z dr, \tag{4.2.28}$$

where $\rho \to \rho_a$ has been adopted, (4.2.8) has been used, and integration over r from r = 0 to $r = \tilde{R}$ has been carried out. Hence,

$$\rho_a \tilde{R}\dot{\tilde{R}} = \int_0^{\tilde{R}/b} \left(\rho_a W b^2\right)_z x e^{-x^2} dx; \tag{4.2.29}$$

if the upper limit is approximated as infinity, then, by (4.2.16),

$$\tilde{R}\dot{\tilde{R}} = \alpha W b. \tag{4.2.30}$$

Thus, from (4.2.27) and (4.2.30),

$$\dot{V} = 2\Omega \alpha W. \tag{4.2.31}$$

Equations (4.2.16), (4.2.18), (4.2.22), (4.2.25), and (4.2.31) constitute five relations for the five dependent variables V, W, σ, f, b. The option of substituting for σ explicitly by means of the algebraic relation (4.2.18), to reduce the number of unknowns and equations by one, is adopted below.

It is convenient to introduce substitute variables as follows:

$$F \equiv \rho_a W b^2, \; G \equiv \rho_a W^2 b^2, \; H \equiv p_a W b^2 \left(\frac{f}{g} - \frac{\sigma}{p_a}\right); \tag{4.2.32}$$

hence,

$$W = \frac{G}{F}, \; b = \frac{F}{(\rho_a G)^{\frac{1}{2}}}, \; f = \frac{g}{(p_a/\rho_a)} \left(\frac{H}{F} + \ell n 2 \; V^2\right). \tag{4.2.33}$$

Equation (4.2.16) becomes

$$\frac{dF}{dz} = 2\alpha \rho_a^{\frac{1}{2}} G^{\frac{1}{2}}. \tag{4.2.34}$$

Equation (4.2.25) becomes

$$\frac{dH}{dz} = -\frac{2}{\gamma} \rho_a^{\gamma-1} \left[\frac{d}{dz} \left(\frac{p_a}{\rho_a^{\gamma}}\right)\right] F. \tag{4.2.35}$$

Equation (4.2.32) becomes, with use of (4.2.34),

$$\frac{dG}{dz} = \frac{2FG}{G^2 + 2(\ell n 2)V^2 \; F^2} \left\{\frac{g}{(p_a/\rho_a)} \left[H + (\ell n 2)V^2 \; F\right] + (\ell n 2)\left[F \frac{dV^2}{dz} + 4\alpha \rho_a^{\frac{1}{2}} G^{\frac{1}{2}} V^2\right]\right\}. \tag{4.2.36}$$

Equation (4.2.31) becomes

$$\dot{V} = 2\Omega \alpha(G/F). \tag{4.2.37}$$

Use of (4.2.8)-(4.2.11) and (4.2.13) in (4.2.1)-(4.2.3) with $\rho \to \rho_a$, yields, from (4.2.27)

$$F(0) = \frac{2}{\pi} M = 0, \quad G(0) = \frac{4}{\pi} \phi = 0, \quad H(0) = \frac{4(\gamma - 1)}{\pi \gamma} E > 0, \qquad (4.2.38)$$

where E is in units of energy per unit time, and F(0) refers to the value of F at z = 0, assigned as the source position.

If one also postulates as an initial condition

$$V(z,0) = 0, \qquad (4.2.39)$$

i.e., no swirl in the flow at time zero, then the formulation is complete. The boundary/initial-value problem consists of the equations (4.2.34)-(4.2.37), subject to the spatial constraints (4.2.38) and the starting condition (4.2.39). It is reiterated that the following is given: the ambient thermodynamic state $p_a(z)$, $\rho_a(z)$; the entrainment parameter α (now probably a <u>function</u> of V); and the ambient angular speed Ω, buoyancy-source strength E, and gas properties such as γ.

The boundary/initial-value problem is nondimensionalized by use of the quantities $\rho_a(0)$, $T_a(0)$, $d\rho_a(0)/dz$, and E, where it is recalled that

$$p_a(0) = \rho_a(0) R\, T_a(0). \qquad (4.2.40)$$

It is convenient to define

$$\varepsilon \equiv \frac{E}{\rho_a(0) c_p\, T_a(0)}, \quad B \equiv \rho_a^{\gamma-1}(0) \frac{d}{dz}\left[\left(\frac{p_a}{\rho_a^{\gamma}}\right)\right]_{z=0}, \qquad (4.2.41)$$

where $d(p_a\, \rho_a^{-\gamma})/dz$ is positive in a dry stable atmosphere, zero in a dry neutrally stable atmosphere, and negative in a dry unstable atmosphere; here, it is taken positive. The units of ε are volume per time; of B, acceleration (length per time squared). Hence, a length scale is furnished by $\varepsilon^{2/5} B^{-1/5}$; a time scale, $\varepsilon^{1/5} B^{-3/5}$; a speed scale, $\varepsilon^{1/5} B^{2/5}$. Thus, if dimensionless quantities are defined by a super bar,

$$\overline{F}(\overline{z};\overline{t}) \equiv \frac{F(z;t)}{\rho_a(0)\varepsilon} \Longrightarrow \overline{F}(0;\overline{t}) = \frac{F(0;t)}{\rho_a(0)\varepsilon} = \frac{2M/\pi}{\rho_a(0)\varepsilon} = 0; \tag{4.2.42}$$

$$\overline{G}(\overline{z};\overline{t}) \equiv \frac{G(z;t)}{\rho_a(0)\varepsilon^{6/5}\, B^{2/5}} \Longrightarrow \overline{G}(0;\overline{t}) = \frac{G(0;t)}{\rho_a(0)\varepsilon^{6/5}\, B^{2/5}} = \frac{4\phi/\pi}{\rho_a(0)\varepsilon^{6/5}\, B^{2/5}} = 0; \tag{4.2.43}$$

$$\overline{H}(\overline{z};\overline{t}) = \frac{H(z;t)}{\rho_a(0)c_p\, T_a(0)\varepsilon} \Longrightarrow \overline{H}(0;\overline{t}) = \frac{H(0;t)}{E} = \frac{4(\gamma - 1)E/(\pi\gamma)}{E} = \frac{4(\gamma - 1)}{\pi\gamma}; \tag{4.2.44}$$

$$\overline{V}(\overline{t};\overline{z}) = \frac{V(t;z)}{\varepsilon^{1/5}\, B^{2/5}} \Longrightarrow \overline{V}(0;\overline{z}) = \frac{V(0;z)}{\varepsilon^{1/5}\, B^{2/5}} = 0; \tag{4.2.45}$$

$$\overline{z} = \frac{z}{\varepsilon^{2/5}\, B^{-1/5}}\ ;\ \overline{t} = \Omega t; \tag{4.2.46}$$

$$\overline{A}(\overline{z}) \equiv \frac{A(z)}{A(0)} = \frac{A(z)}{B} = \frac{\left[\rho_a(z)\right]^{\gamma-1} \frac{d}{dz}\left(\frac{p_a}{\rho_a^{\gamma}}\right)}{B}\ . \tag{4.2.47}$$

The order of arguments in $\overline{F}$, $\overline{G}$, $\overline{H}$ reflects the explicit dependence on $\overline{z}$, the parametric dependence on $\overline{t}$; the order of arguments in $\overline{V}$, $\overline{\sigma}$ reflects the reversed roles. On the basis of comments below (4.2.41), $\overline{A}(\overline{z}) > 0$ for a stable atmosphere. For the special case of neutral stability, $\overline{A}(\overline{z}) = 0$, and $B = 0$ as well; for this special case (of limited physical interest), H is constant from (4.2.35), and an individualized treatment is appropriate.

From (4.2.18)-(4.2.19), (4.2.33), and (4.2.42)-(4.2.45), the basic dependent variables are expressed as follows:

$$\overline{W}(\overline{z};\overline{t}) \equiv \frac{W(z;t)}{\varepsilon^{1/5}\, B^{2/5}} = \frac{\overline{G}(\overline{z};\overline{t})}{\overline{F}(\overline{z};\overline{t})}\ ; \tag{4.2.48}$$

$$\overline{b}(\overline{t};\overline{z}) \equiv \frac{b(z;t)}{\varepsilon^{2/5}\, B^{-1/5}} = \frac{\overline{F}(\overline{z};\overline{t})}{\left[\overline{\rho}_a(\overline{z})\right]^{1/2}\left[\overline{G}(\overline{z};\overline{t})\right]^{1/2}}\ ; \tag{4.2.49}$$

$$\bar{\sigma}(\bar{t};\bar{z}) \equiv \frac{\sigma(t;z)}{\rho_a(0)\varepsilon^{2/5}\, B^{4/5}} = (\ell n 2)\left[\bar{\rho}_a(\bar{z})\right]\left[\bar{V}(\bar{t};\bar{z})\right]^2; \tag{4.2.50}$$

$$\bar{f}(\bar{z};\bar{t}) \equiv \frac{f(z;t)}{g} = \frac{\gamma}{\gamma - 1}\,\frac{\bar{\rho}_a(\bar{z})}{\bar{p}_a(\bar{z})}\left\{\frac{\bar{H}(\bar{z};\bar{t})}{\bar{F}(\bar{z};\bar{t})} + (\ell n 2)(E_c)\left[\bar{V}(\bar{t};\bar{z})\right]^2\right\}, \tag{4.2.51}$$

where

$$\bar{\rho}_a(\bar{z}) \equiv \frac{\rho_a(z)}{\rho_a(0)}\ ,\ \bar{p}_a(\bar{z}) \equiv \frac{p_a(z)}{p_a(0)}\ ,\ Ec \equiv \frac{\varepsilon^{2/5}\, B^{4/5}}{c_p(0)T_a(0)}\ , \tag{4.2.52}$$

where the Eckert number Ec as defined here is <u>not</u> a conventional ratio of kinetic to thermal energy, and hence is retained even for the highly subsonic flows of interest.

Equations (4.2.34)-(4.2.39) are now expressed in terms of dimensionless variables and parameters introduced in (4.2.42)-(4.2.47), (4.2.52):

$$\frac{d\bar{F}}{d\bar{z}} = 2\alpha\,\bar{\rho}_a^{\,1/2}\,\bar{G}^{\,1/2}; \tag{4.2.53}$$

if

$$Gr \equiv \frac{\gamma}{\gamma - 1}\,\frac{g}{B}\ , \tag{4.2.54}$$

$$\frac{d\bar{G}}{d\bar{z}} = \frac{2\bar{F}\,\bar{G}}{\bar{G}^2 + 2(\ell n 2)(\bar{F}\,\bar{V})^2}\left\{(Gr)\,\frac{\bar{\rho}_a}{\bar{p}_a}\left[\bar{H} + (\ell n 2)(Ec)\bar{V}^2\,\bar{F}\right]\right.$$

$$\left. + (\ell n 2)\left[\bar{F}\,\frac{d\bar{V}^2}{d\bar{z}} + 4\alpha\,\bar{V}^2\left(\bar{\rho}_a\,\bar{G}\right)^{1/2}\right]\right\}; \tag{4.2.55}$$

$$\frac{d\bar{H}}{d\bar{z}} = -\,\frac{2}{\gamma}\,(Ec)\bar{A}\,\bar{F}\,; \tag{4.2.56}$$

$$\frac{d\bar{V}}{d\bar{t}} = 2\alpha\,\frac{\bar{G}}{\bar{F}}\ . \tag{4.2.57}$$

These equations are to be solved subject to (4.2.42)-(4.2.45). The entrainment functional α is anticipated to decrease as $\overline{V}$, or perhaps $\overline{b}\,\overline{V}$, increases; empiricism is required to establish the functional, and only very preliminary and limited data is available (Ying 1965). While in general atmospheric soundings with hydrostatics yield appropriate forms for $\overline{p}_a(\overline{z})$, $\overline{\rho}_a(\overline{z})$ and, hence for $\overline{A}(\overline{z})$, a one-parameter basis of comparison of the effect of stratification also is carried out for the (artificial) class of atmospheres $\overline{p}_a(z) = [\overline{\rho}_a(\overline{z})]^{\kappa\gamma}$, $1 > \kappa > 0$, such that

$$\overline{A}(\overline{z}) = -\left[\overline{\rho}_a(\overline{z})\right]^{\kappa\gamma-2}\left(\frac{d\rho_a(z)}{dz}\right)\Bigg/\left|\frac{d\rho_a(0)}{dz}\right| \quad , \; 1 > \kappa > 0 \; , \tag{4.2.58}$$

where $\overline{A}(\overline{z}) > 0$ since $[d\rho_a(z)/dz] < 0$ and where $\overline{\rho}_a(\overline{z})$, drawn from any plausible source, is held invariant as κ is altered. While it is well known that inversion layers (in which the temperature increases with increasing altitude) do arise occasionally in the lower troposphere, in general the temperature decreases as altitude increases in the troposphere, such that the inequality $1 > \kappa > \gamma^{-1}$ provides more realistic bounds. In preliminary investigation κ is held constant over all z; more realistic stratification may be achieved by taking κ as piecewise constant over intervals of $\overline{z}$. Incidentally, since firestorm environments are in general very dry, the neglect of water vapor in the discussion of atmospheric stratification is more suitable here than would be the case in other contexts.

The method of solution is implied in earlier discussions of explicit and parametric dependence, and in the (cavalier) use of total derivatives in the differential equations. The three equations with a first spatial derivative are integrated in the sense of increasing $\overline{z}$ (until $\overline{W} \to 0$) by use of the boundary conditions at $\overline{z} = 0$; at $\overline{t} = 0$, the classical solution for a nonrotating plume, with $\overline{\sigma} = \overline{V} = 0$ for all $\overline{z}$, is obtained as a starting profile. The one equation with a temporal derivative is then stepped forward in time at each $\overline{z}$. The three first-spatial-derivative equations are then integrated with the same time-invariant conditions holding at $\overline{z} = 0$, but with finite value for $\overline{V}$ (and $\overline{\sigma}$) at all $\overline{z}$. Sequential repetition ensues. Numerical experimentation is relied upon to ascertain

adequate refinement of the spatial mesh and (of particular concern) the temporal interval for the finite-difference approximations.

Analytic expressions are required as $\bar{z} \to 0$ because of the singularity at the point source; substitution of series gives

$$\bar{F} = f_1 \bar{z}^{5/3} + \ldots , \tag{4.2.59}$$

$$\bar{G} = g_1 \bar{z}^{4/3} + \ldots , \tag{4.2.60}$$

$$\bar{H} - h_o = h_1 \bar{z}^{8/3} + \ldots , \tag{4.2.61}$$

where

$$h_o = \frac{4}{\pi} \frac{(\gamma - 1)}{\gamma} , \; f_1 = \frac{6}{5} \alpha g_1^{1/2}, \; h_1 = - \frac{9}{10} \left(\frac{Ec}{\gamma} \right) \alpha g_1^{1/2}; \tag{4.2.62}$$

$$\bar{V} = \frac{5}{3} g_1^{1/2} \bar{z}^{-1/3} \bar{t} + \ldots ; \tag{4.2.63}$$

$$g_1 = \left[\frac{9(Gr)h_o \alpha}{5} \right]^{2/3} \left[1 - 8(\ell n 2)\alpha^2 \bar{t}^2 \right]^{-2/3} . \tag{4.2.64}$$

From (4.2.48), (4.2.49), and (4.2.51), these expressions imply that as $\bar{z} \to 0$,

$$\bar{W} \sim \frac{5}{6} \frac{g_1^{1/2}}{\alpha} \bar{z}^{-1/3}, \; \bar{b} \sim \frac{6}{5} \alpha \bar{z},$$

$$\bar{f} \sim \frac{\gamma}{\gamma - 1} \left[\frac{5 h_o}{6 \alpha g_1^{1/2}} \bar{z}^{-5/3} + \frac{25}{9} (\ell n 2)(Ec) g_1 \bar{z}^{-2/3} \bar{t}^2 \right] . \tag{4.2.65}$$

These asymptotic forms hold at all $\bar{z}$ for a nonrotating, neutrally stable ambient, if one discards the term containing $\bar{t}^2$ in the expression for $\bar{f}$ and discards the term containing $\bar{t}^2$ in the expression for g_1. Explicitly, as $\bar{z} \to 0$, $\bar{H} \sim h_o \doteq 4(\gamma - 1)/(\pi\gamma)$, and

$$\overline{W} \sim \frac{5}{6}\frac{g_1^{1/2}}{\alpha_0}\,\overline{z}^{-1/3}\,,\quad \overline{b} \sim \frac{6}{5}\,\alpha_0\,\overline{z},\quad \overline{f} \sim \frac{\gamma}{\gamma-1}\,\frac{5\,h_0}{6\,\alpha_0\,g_1^{1/2}}\,\overline{z}^{-5/3}\,,$$

$$g_1 = \left[\frac{9(Gr)h_0\,\alpha_0}{5}\right]^{2/3}\,, \qquad (4.2.66)$$

where α has been set equal to α_0, the nonrotating-ambient value of the entrainment constant. The linear growth of the plume dimension $\overline{b}$, the relatively weak singularity in $\overline{W}$, and the relatively strong singularity in $\overline{f}$ are noteworthy. The asymptotic forms of (4.2.66) are used (somewhat arbitrarily) to initiate the solution for small $\overline{z}$ at any fixed $\overline{t}$; the solution is continued to larger $\overline{z}$ via (4.2.53)-(4.2.56), with the aid of (4.2.28)-(4.2.51).

Conventionally the relations (4.2.66) are used to assign a "subterranean" location to the ("virtual") point source of heat release, such that the plume width $\overline{b}$ assumes the (known) finite dimension of the actual ground-level source. That is, assignment of the nondimensionalized source width $\overline{b}_{finite}$ identifies the axial distance $\overline{z}_0$ that the ground lies above the virtual source at $\overline{z} = 0$. Actually, since the equations are translationally invariant in $\overline{z}$, for convenience one may take the ground level as $\overline{z} = 0$ by letting $\overline{z} \to (\overline{z} + \overline{z}_0)$, where $\overline{b}_{finite} = (6/5)\alpha_0\,\overline{z}_0$, such that the equivalent point source lies at $(-\overline{z}_0)$. In any case, assigning $\overline{W},\overline{f}$ at ground level by taking the domain between the point source and the finite source as an adiabatic, nonrotating domain seems as plausible as any alternative procedure. The fact is that integral-plume theory can be expected to give quantitatively accurate results only in the far field, where the finite source acts effectively as a point source, and correlating the point source with a finite-dimension source cannot be expected to result in the theory yielding quantitatively accurate description near the finite source. Thus, here no highly painstaking attempt is made to locate a virtual point source to correlate with a finite-dimension source.

4.3 Assignment of Parameter Values; Properties of the Solution

It is taken that the virtual source position $\bar{z}_0$ is finite so that numerical integration may commence at $\bar{z} = 0$. If one adopted meteorological convention (Cole 1975), z_0 would be taken as 10 m, such that $\bar{z} = 0$ would be the standard height of "surface wind" measurement. However, such a convention is not adopted with the highly exceptional case of a firestorm in mind. If (rather arbitrarily) $b_{finite} \doteq 0.1$ km, then from (4.2.66) $z_0 \doteq 1$ km; for $\kappa = 0.97$, $\gamma = 1.4$, $T_a(0) = 300$ K, $\rho_a(0) = 1.16 \times 10^{-3}$ g/cm^3, $\varepsilon = O(10^{10}$ cm^3/s), $B = O(85$ cm/s$^2)$, the typical wind speed scale $\varepsilon^{1/5} B^{2/5} = O(5$ m/s), the typical length scale $\varepsilon^{2/5} B^{-1/5} = O(50$ m), and from (4.2.66) the typical vertical wind speed at "ground level" $z = 0$ is $W = O(25$ m/s). This updraft speed is typical of the speeds found in the undiluted cores of cumulonimbi (Fendell 1974) and seems not an implausible value to expect in the lower portion of a firestorm plume.

The value $\varepsilon = O(10^{10}$ cm^3/s), discussed in the previous paragraph, is attained thus. In the Hamburg firestorm, about 12 km^2 of the Hammerbrook residential section, with combustible-fuel loading of 157 kg/m^2 with heating value of $O(2 \cdot 10^{11}$ ergs/gm), burned rather completely. Hence, very roughly $4 \cdot 10^{22}$ ergs could have been released. If $\varepsilon = O(10^{10}$ cm^3/s), then $E = O(3 \cdot 10^{16}$ ergs/s), and, in 6 hours, $6 \cdot 10^{20}$ ergs would be released. Thus, $\varepsilon = O(10^{10}$ cm^3/s) is (barely) compatible with the available exothermicity.

For an atmosphere in which $p_a \sim \rho_a^{\kappa\gamma}$ [see above (4.2.58)],

$$\frac{dT_a}{dz} = -\left[\frac{\kappa\gamma - 1}{\kappa(\gamma - 1)}\right] \frac{g}{c_p} \tag{4.3.1}$$

by use of the state law, hydrostatics, and $p_a \sim \rho_a^{\kappa\gamma}$. At the Hamburg airport at the time of the firestorm, between 300 m and 3000 m,

$$\frac{\kappa\gamma - 1}{\kappa(\gamma - 1)} \doteq 0.87 \Longrightarrow \kappa \doteq 0.95. \tag{4.3.2}$$

A significantly higher value of κ almost surely held in Hammerbrook itself, and the value $\kappa = 0.97$ was cited above. (In the Darwin fire cited in Section 1.3, $\kappa = 0.86$ to 6000 m.)

The value of B, from (4.2.47) and the relation above (4.2.58) is given by

$$B = -\gamma(1 - \kappa) \frac{p_a(0)}{[\rho_a(0)]^2} \frac{d\rho_a(0)}{dz} , \qquad (4.3.3)$$

or $B = O(0.2\ m/s^2)$ for $\kappa = 0.995$, $B = O(0.5\ m/s^2)$ for $\kappa = 0.96$.

The low-level swirl speeds compatible with the model are, from (4.2.31) and (4.2.35), with α and W constant at $z = 0$, if V_0 is the initial value of V,

$$V - V_0 = (2\Omega t)(\alpha W).$$

But $\Omega \doteq (6h)^{-1}$ at midlatitudes, if Ω is based on the component of the rotation of the earth locally normal to a tangent plane. Also, 3 hours characterizes the time t of interest. Hence, $(V - V_0) \doteq \alpha W$. But $\alpha \doteq 0.1$, and accounting for swirl of the ambient decreases α, so at most $(V - V_0)$ is an order of magnitude smaller than W after 3 hours of persistence of convection. If (say) $W = 30$ m/s near $z = 0$, then $(V - V_0) = 3$ m/s. From solution of the nonlinear inflow layer under a vortex, the peak value of the surface-layer inflow speed u is O(v), and from (4.2.11) the peak value of v occurs at $(r/b) \doteq 1.11$ where $v \doteq 0.64\ V$. That is, the peak value of both u and v is about 2 m/s if V_0 is zero.

There are four considerations concerning these relatively small values of swirl and inflow that warrant mention. First, estimates of 25-50 m/s radial influx are pure guesses made by observers in the midst of a holocaust. Second, for fuel loadings of 100 kg/m^2 or so in construction extending but a few stories, one recognizes the presence of small thorough fares joining larger boulevards. As the width of a thorough fare decreases, the wind speed increases, for the highly subsonic flows of interest. Hence, the larger values, if valid at all, are likely to pertain to narrower side streets. Third, the background angular speed could be enhanced appreciably over that of the rotation of the earth, such that Ω might be ascribed values several times that given above, which was $(6h)^{-1}$. Fourth, the value of the swirl at the initiation of convection may well have been 4 m/s at Hamburg; in fact, a far brisker wind existed throughout the firestorm event at

Dresden, and the fact that a vertical plume was observed suggests strongly that a cyclonic rotation (rather than a cross-wind) preceded, and persisted throughout, the firestorm event. Thus, if V_∞ = 4 m/s and $\Omega = (2h)^{-1}$, then near the surface after 3h the value of V is 13 m/s; the associated radial influx is then 9 m/s, and if an augmentation by a factor of three or four owing to constriction on narrower streets, then all but the highest reported values seem plausible. What seems clear is that estimates of 25-50 m/s seem not to be conservative, and might overestimate somewhat what wind speeds have ariser in the past or are likely to arise in the future. Perhaps it is apropos to cite the significant inflation of some wind-speed estimates in tornadoes, made not just by laymen; these inflated values [some approaching sonic speed (!)] exceed appreciably the speeds attainable under even idealizations of known atmospheric processes.

If one generalizes the initial condition (4.2.45), so that

$$\overline{V}(0;\overline{z}) = \overline{T}(\overline{z}), \text{ given,} \qquad (4.3.4)$$

then at time zero the starting structure of the plume is not the classical one. From inspection of (4.2.5) under the cyclostrophic approximation and of (4.2.6), one sees that for axial positions for which the swirl increases with altitude, the pressure decrement from hydrostatic owing to swirl leads to an axial pressure gradient that acts to enhance axial acceleration arising from buoyancy (i.e., a density discrepancy relative to ambient). However, for axial positions for which the swirl decreases with altitude, the pressure decrement from hydrostatic owing to swirl acts to reduce axial acceleration from buoyancy. Since $W_z < 0$ at least at large height, and since $V_t \sim W$, one expects an even more rapid deceleration of ascent if the plume rises in a rotating ambient. If entrainment α is not altered by the presence of swirl, i.e., if one takes $\alpha = \alpha_0$ even for V finite, and if $W_z < 0$ for all z (and it is recalled that $W \sim z^{-1/3}$ for all z for an adiabatic nonrotating atmosphere), then the effect of ambient rotation is likely to be a lower height to the plume, relative to the altitude at which $W \to 0$ for the same parametric assignments except $\Omega = 0$.

Below (4.2.39) it was stated that α probably decreases significantly from the value α_0 as V achieves significant magnitude (Ying 1965). Clearly,

not only the rate at which ambient mass is entrained (as reflected in α), but also the buoyancy-reducing effect of that entrainment (as reflected in <) enters into deliberation, for fixed values of ε, ', etc. Nevertheless, it may be anticipated that appreciable decrement in the entrainment parameter α results in the plume achieving substantially greater altitude. On the other hand, if spin-up begins to result in a reduction of the entrainment parameter α, from (4.2.57) such reduction of α limits further spin-up. Hence swirl speeds may not attain even the modest values cited earlier on the basis of ascribing to α the constant value α_0, where empirically $\alpha_0 = 0.093$. If the swirl is small, then the cyclostrophic balance is a less accurate statement of the conservation of radial momentum. But the cyclostrophic balance is a mechanistic explanation of the reduction of entrainment in a swirling ambient, a reduction that usually results in a higher plume. Hence, one expects a threshold of swirl above which entrainment is reduced, but below which entrainment is effectively unaltered. The following form is set forth for trial:

$$\alpha = \alpha_0 \exp\left\{- c(\overline{V} - \overline{V}_0)^n U(\overline{V} - \overline{V}_0)\right\} , \qquad (4.3.5)^*$$

where c, $\overline{V}_0$, $n > 0$ and the Heaviside unit step function is defined by

$$U(x) = 0,\ x < 0;\ U(x) = 1,\ x > 0;\ U(x) = \tfrac{1}{2},\ x = 0. \qquad (4.3.6)$$

---

*In the parlance of geophysical fluid dynamics for a noninertial coordinate system rotating with the earth, entrainment is taken as effectively unmodified for small or moderate Rossby number (such that geostrophy or the gradient-wind equation, perhaps even supplemented with radial advection, adequately describes the conservation of radial momentum); however, entrainment is taken as significantly modified (i.e., reduced) for larger Rossby number (such that cyclostrophy suffices as a statement of conservation of radial momentum). Emmons and Ying (1967), while inferring an order of magnitude decrease in α for a laboratory firewhirl experiment for peak ambient swirl of order 60 cm/s, infer a 35% increase in α for peak ambient swirl of order 10 cm/s. However, this increase might be attributable to vortex breakdown, so the conservative procedure followed here is to leave the entrainment constant unaltered for small swirling speed. Incidentally, in terms of the functional form introduced in (4.3.5) the values inferred by Emmons and Ying suggest $c = O(50)$ for $(\overline{V} - \overline{V}_0) \doteq 0.2$.

One could devise an expression in which α would be very slightly decremented for $\overline{V} < \overline{V}_0$ below and appreciably decremented for $\overline{V} > \overline{V}_0$; e.g., for $n > 0$, $1 >> \overline{\varepsilon} > 0$, one might take

$$\alpha = (\alpha_0/2)\left[\text{erfc}\left(\frac{\overline{V} - \overline{V}_0}{\overline{\varepsilon}}\right)^n\right]. \qquad (4.3.7)$$

However, in the absence of experimental data, (4.3.5) would seem as adequate a basis of numerical experimentation as any alternative. One anticipates $V_0 > \max[T(z)]$, but V_0 is modest [say, O(3 m/s)]. One observational implication of (4.3.5) is that some degree of spin-up occurs before any increase in plume height occurs. But once the plume height begins to rise (i.e., for $\overline{V} > \overline{V}_0$ so $\alpha < \alpha_0$), then further spin-up become gradually ever more retarded. Incidentally, it may be noted that the plume concept is degenerate in the case of $\alpha = 0$, and $\alpha = 0$ is not achieved at any finite $\overline{V}$ in the forms discussed here.

If ε characterizes the <u>initial</u> rate of heat release by combustion, but that rate changes in time, the suggestion here is that the adopted "time-splitting" approach suffices to accomodate such change, provided the change is not too rapid. The time for a particle to rise a height $\overline{z}$ can be obtained from (if $\overline{z}_{TOP}$ denotes the dimensionless height at which $\overline{W}$ decreases to a preset small value)

$$\frac{dz}{dt} = W(z;t) \Rightarrow \overline{t}_{rise}(\overline{t}) = \Omega\, \varepsilon^{1/5}\, B^{-3/5} \int_0^{\overline{z}_{TOP}} \left[\overline{W}(x_1;\overline{t})\right]^{-1} dx_1 . \qquad (4.3.8)$$

The value of h_0 should not change by much more that 10% over the time interval $\overline{t}_{rise}$, which varies with $\overline{t}$. For simplicity, if the average ascent speed is 10 m/s and if the plume extends to 10 km, then t_{rise} is about a quarter hour. In 1 hour, the value of h_0 could be reduced to roughly two-thirds of its value <u>if</u> the ratio of plume height to average ascent speed remained roughly fixed with decreasing h_0. These comments touch upon the matter of how the present theory could be adapted to describe the first weakening of a firestorm, although, since $V_t > 0$, there is no provision for spin-down.

Attention is now turned to numerical experimentation with values for $\overline{b}_{finite}$ (or $\overline{z}_0$), c, $\overline{V}_0$, n, $\overline{T}(\overline{z})$, as well as for κ, Gr, Ec, γ, and $\overline{\sigma}_a(\overline{z})$, and for the (variable) time interval ($\Delta\overline{t}$) and (variable) space interval ($\Delta\overline{z}$) that suffices for current purposes. Simple forward Euler differencing is used in time, with doubling of ($\Delta\overline{t}$) from a small initial value whenever the maximum percentage change in $\overline{V}$ at any $\overline{z}$ over the last time interval is less than some prescribed fractional value. Also, the calculation is terminated on the condition that $\overline{W}$ has decreased to some small but finite value, such as $\overline{W} = 0.1$, since $\overline{b} \to \infty$ as $\overline{W} \to 0$ and there is virtually no physical content to be derived from the difficult numerical exercise of proceeding to indefinitely small $\overline{W}$; as $\overline{W}$ decreases in $\overline{z}$, $\overline{V}$ decreases and $\overline{f}$ will have already become negative (decelerating buoyancy).

4.4 Numerical Results

The following values of the input parameters determine the nominal case:

$$\varepsilon = 1.0 \cdot 10^{10} \text{ cm}^3/\text{s},\ \varkappa = 0.98,\ \gamma = 1.4,\ \alpha_o = 0.093,\ b_{finite} = 0.1 \text{ km},$$

$$c = 100,\ \bar{V}_o = 0.55,\ n = 2,\ \bar{T}(\bar{z}) = 0,\ p(0) = 1.0 \cdot 10^5 \text{ N/m}^2,$$

$$\rho(0) = 1.16 \cdot 10^{-3} \text{ g/cm}^3,\ \Omega = (6 \text{ h})^{-1}. \qquad (4.4.1)$$

In this notation $p(0)$ and $\rho(0)$ refer to their respective values at the ground $z = 0$. The virtual source is located below the ground at a position $-z_o$.

These nominal case input values result in the following derived quantities:

$$B = 0.246 \text{ m/s}^2,\ Gr = 139.6,\ Ec = 4.312 \cdot 10^{-5},$$

$$T_a(0) = 300.4 \text{ K},\ z_o = 0.896 \text{ km}. \qquad (4.4.2)$$

In addition, the typical length scale $\varepsilon^{2/5} B^{-1/5} = 52.7$ m and the typical wind speed scale $\varepsilon^{1/5} B^{2/5} = 3.6$ m/s.

For ease of gathering data at specified times, a constant step size of $(\Delta\bar{t}) = 0.01$ is employed. The calculation is terminated at $\bar{t}_f = 0.8$, or $t_f = 4.8$ h since $t = \Omega^{-1} \bar{t}$ with $\Omega = (6 \text{ h})^{-1}$.

In Figures 1-4 the computed profiles for swirl speed V, updraft speed W, plume width b, and dimensionless density discrepancy $\bar{f}$ are presented for the nominal case at several values of time. The height of the column, determined by $W \to 0$, is 3.94 km at $t = 0$. For the first 3 hours, during which $\bar{V} < \bar{V}_o$ so that $\alpha = \alpha_o$, the swirl speed V builds up while the other profiles remain essentially invariant.

For $t > 3$ hours, $\bar{V} > \bar{V}_o$ (at least for z near z_o), and hence $\alpha < \alpha_o$. In this time interval, the column height increases with time; the swirl at z_o increases with time but its rate of increase diminishes; the updraft

W develops a nonmonotonic "bulge" such that the maximum W occurs at a "mid-altitude". The plume-width profiles exhibit a more vertical slope at lower altitudes and rise higher to nearly the total column height before "bending" to $(db/dz) \to \infty$. The density discrepancy $\bar{f}$ monotonically decreases with altitude. For $4.8 \geq t(h) \geq 0$ inclusive, the point $\bar{f} = 0$ is reached at a altitude approximately 7/10 of the column height.

The results of parametric variation of the input quantities are presented in Table 1. Except for those values explicitly denoted, input parameters are those of the nominal case (4.4.1). The table presents results for: z_f, the top of the column, at $t = 0$ and $t = 4.8$; $B(m/s^2)$; $W(0)$, the updraft at $z = 0$; W_{max}, the maximum updraft at z for $t = 4.8$; $z(w_{max})$, the altitude at which W_{max} occurs; V_{max}, the swirl at $z = 0$ for $t = 4.8$; $z|_{\bar{f}=0}$, the altitude at which $\bar{f} = 0$ for $t = 0$ and the analogous altitude for $t = 4.8$; t_{rise}, the time for a particle to rise the height of the column. This last quantity is presented at $t = 0$ and at $t = 3.0$. The rise time in a typical case increases slowly in the domain $0 \leq t \leq 3.0$, then decreases slowly in the domain $3.0 \leq t \leq 4.8$.

5. DIRECTIONS FOR FURTHER DEVELOPMENT

5.1 Generalizations

Several directions for fruitful investigation may be anticipated. As already noted, one needed input is accessible by experiment only: determining the decrement of the entrainment functional with increasing rotation of the ambient through which the ascent of the buoyant plume (from the maintained heat source) occurs. Laboratory experimentation with a pool fire within a rotating screen may well be adequate for this insight. Also already noted is another needed input of a theoretical nature: accomodating at the base of the plume an evolving, swirl-induced input of mass flux and momentum flux, to complement the more conventional buoyancy flux. These fluxes arise from the surface inflow layer engendered on a relatively nonrotating ground plane supporting a rapidly swirling flow.

Here some further very preliminary and very tentative comments are added on still another topic previously mentioned: providing the theory with enough resolution to allow for the possible ("worst-case") development of a downward motion (an eye), a development which is exluded a priori under existing integral models of gravitational convection. The suggestion is made here that the following novel form for the vertical velocity component be introduced:

$$w(r,z) = W_1(z)\,\exp\left[-r^2/b^2(z)\right] + W_2(z)\exp\left\{-\left[r - a(z)\right]^2/c^2(z)\right\}, \quad (5.1.1)$$

where conventionally $W_1(z) > 0$, $W_2(z) = 0$, for all z. Here, the possibility that $W_1(z) < 0$, $W_2(z) > 0$, for some (large) values of z is accomodated, with b(z) characterizing "eye" thickness, a(z) characterizing "eyewall" displacement from the axis of symmetry and of rotation, and c(z) characterizing "eyewall" thickness. While continuity in the low-Mach-number-approximation form

$$\frac{\partial(\rho_a\, r\, u)}{\partial r} + \frac{\partial(\rho_a\, r\, w)}{\partial z} = 0 \quad (5.1.2)$$

would yield u(r,z), given w(r,z), without introduction of any new unknowns, the above expression for w(r,z) contains three more unknowns than does the

conventionally adopted expression. Clearly, one must extract more from each conservation equation than one ordinary differential equation in order to obtain a determinate system.

It seems plausible that v(r,z) be obtained from conservation of angular momentum. It further seems plausible to hypothesize that, if in general

$$\rho\, r\, v_t + 2\Omega\, \rho\, r\, u + \rho\, u(rv)_r + \rho\, w(rv)_z = 0, \qquad (5.1.3)$$

where subscripts t, r, z denote partial differentiation, in $r > a(z)$, only the first two terms need be retained in the lowest-order approximation. In fact in $r > [a(z) + c(z)]$, the <u>outer</u> swirl seems adequately described by

$$\rho_a\, r\, v_t + 2\Omega\, \rho_a\, r\, u \doteq 0. \qquad (5.1.4)^*$$

Initially v(r,z,t) is very small, i.e., $\Omega\, r$; for later times, a perturbation on $\Omega\, r$ may be introduced. This outer swirl implies a surface-layer influx that in turn implies a finite mass source and a finite axial momentum source into the flow just above the surface layer (see above).

At this point it seems that (1) the profiles for u(r,z) and v(r,z) must be closely related in order to render the number of unknowns equal to the number of equations; (2) the pressure p(r,z) may be obtained from the conservation of angular momentum; and (3) the energy and axial momentum equations may then be considered, though a bimodal form seems appropriate for the density discrepancy from ambient.

Morton et al (1956, p. 6) comment that "... the fluid in the topmost part of the plume will fall back some distance as it spreads sideways, although the solution cannot be expected to show this." While descent

*Approximating (5.1.3) as (5.1.4) results in the relation (4.2.31). As noted in the text, this approximation suffices only in the far field; in the analysis of Section 4 the approximation (5.1.4) effectively has been adopted throughout the flow, and this step seems the major reason why rather modest levels of swirling are generated in the analysis. With retention of radial and axial inertial transport of angular momentum, together with a modest initial swirl (locally enhanced above the rotation associated with the earth), appreciably higher swirling speeds may be anticipated. The tasks implicit in the comments of this footnote may well warrant highest priority on any future agenda.

within the convective plume did not warrant pursuit in the classical context, the known role of the eye in tropical cyclones suggests that provision for two-cell structure in the context of a rotating ambient does warrant consideration. Despite the very rudimentary conjectures given here, perhaps enough has been presented to suggest that some variant of integral theory for convective-plume description may well admit generalization to incorporate two-cell structure.

REFERENCES

Anderson, H. E. 1968 Sundance fire: an analysis of fire phenomena. Res. paper INT-56, Intermountain Forest and Range Exp. Station. Ogden, UT: Forest Service, U.S. Dept. of Agriculture.

Atallah, S. 1966 Some observations on the great fire of London, 1666. Nature 211, 105-106.

Barcilon, A. 1967 Vortex decay over a stationary boundary. J. Fluid Mech. 27, 155-175.

Benech, B. 1976 Experimental study of an artificial convective plume initiated from the ground. J. Appl. Meteorol. 15, 127-137.

Bond, H., ed. 1946 Fire and the Air War. Boston, MA: National Fire Protection Association.

Brandes, E. 1978 Mesocyclone evolution and tornadogenesis. Monthly Weather Rev. 106, 995-1011.

Brode, H. L. 1980 Large-scale urban fires. Note 348. Santa Monica, CA: Pacifica-Sierra Res. Corp.

Broido, A. 1960 Mass fires following nuclear attack. Bull. Atomic Scientists 16, 409-413.

Brown, A. A. and Davis, K. P. 1973. Forest Fire: Control and Use, 2nd ed. New York, NY: McGraw-Hill.

Bureau of Social Affairs, Home Office 1926 The Great Earthquake of 1923 in Japan. Tokyo, Japan: Imperial Japanese Government.

Burggraf, O. R., Stewartson, K., and Belcher, R. 1971 Boundary layer induced by a potential vortex. Phys. Fluids 14, 1821-1833.

Busch, N. F. 1962 Two Minutes to Noon. New York, NY: Simon and Schuster.

Byram, G. M. and Martin, R. E. 1962 Fire whirlwinds in the laboratory. Fire Control Notes 23, 13-17.

Caiden, M. 1960 The Night Hamburg Died. New York, NY: Ballantine.

Carrier, G. F. 1971a Swirling flow boundary layers. J. Fluid Mech. 49, 133-144.

Carrier, G. F. 1971b The intensification of hurricanes. J. Fluid Mech. 49, 145-158.

Carrier, G. F. and Fendell, F. E. 1978 Analysis of the near-ground wind field of a tornado with steady and spatially varying eddy viscosity. Wind Field and Trajectory Models for Tornado-Propelled Objects (EPRI Project 308, Rept. NP-748), pp. A-1--A-45. Palo Alto, CA: Electric Power Res. Inst.

Carrier, G. F., Hammond, A. L., and George, O. D. 1971 A model of the mature hurricane. J. Fluid Mech. 47, 145-170.

Cate, J. L. and Craven, W. F., eds. 1953 The Army Air Forces in World War II. Vol. 5: The Pacific-Matterhorn to Nagasaki, June 1944 to August 1945. Chicago, IL: U. Chicago.

Church, C. R., Snow, J. T., and Dessens, J. 1980 Intense atmospheric vortices associated with a 1000 MW fire. Bull. Amer. Meteorol. Soc. 61, 682-694.

Cole, F. W. 1975 Introduction to Meteorology, 2nd ed. New York, NY: John Wiley.

Committee for the Compilation of Materials on Damage Caused by the Atomic Bombs in Hiroshima and Nagasaki 1981 Hiroshima and Nagasaki. New York, NY: Basic Books.

Countryman, C. M. 1971 Fire whirls -- why, when, where. Rept., Forest Fire Lab., Pacific SW Forest and Range Exp. Station. Berkeley, CA: Forest Service, U.S. Dept. of Agriculture.

Davies-Jones, R. and Kessler, E. 1974 Tornadoes. Weather and Climate Modification, chptr. 16, pp. 552-595. New York, NY: John Wiley.

Davison, C. 1931 The Japanese Earthquake of 1923. London, England: Thomas Murby.

Defense Civil Preparedness Agency 1973 What the planner needs to know about fire ignition and spread. DCPA Attack Environment Manual, chptr. 3. Document CPG 2-1A3. Washington, D.C.: Defense Civil Preparedness Agency.

Dergarabedian, P. and Fendell, F. 1967 Parameters governing the generation of free vortices. Phys. Fluids 10, 2293-2299.

Dessens, J. 1962 Man-made tornadoes. Nature 193, 13-14.

Dessens, J. 1964 Man-made thunderstorms. Discovery 25, 40-44.

Ebert, C. H. V. 1963 The meteorological factor in the Hamburg fire storm. Weatherwise 16, 70-75.

Emmons, H. W. 1965 Fundamental problems of the free burning fire. Tenth Symposium (International) on Combustion, pp. 951-964. Pittsburgh, PA: Combustion Institute.

Emmons, H. W. and Ying. S.-J. 1967 The fire whirl. Eleventh Symposium (International) on Combustion, pp. 475-488. Pittsburgh, PA: Combustion Institute.

Fendell, F. E. 1974 Tropical cyclones. Advances in Geophysics, vol. 17, pp. 1-100. New York, NY: Academic.

Futrell, R. F., Moseley, L. S., and Simpson, A. F. 1961 The United States Air Force in Korea 1950-1953. New York, NY: Duell, Sloan and Pearce.

Glasstone, S. and Dolan, P. J., eds. 1977 The Effects of Nuclear Weapons, 3rd ed. Washington, D.C.: U.S. Dept. of Defense and U.S. Dept. of Energy.

Graham, H. E. 1952 A firewhirl of tornadic violence. Weatherwise 5, 59-62.

Graham, H. E. 1955 Fire whirlwinds. Bull. Amer. Meteorol. Soc. 36, 99-103.

Hanna, S. R. and Gifford, F. A. 1975 Effects of energy dissipation at large power parks. Bull. Amer. Meteorol. Soc. 56, 1069-1076.

Hill, Jerald E. 1961 Problems of fire in nuclear warfare. Rept. P-2414. Santa Monica, CA: Rand Corp.

Hissong, J. E. 1926 Whirlwinds at oil-tank fire, San Luis Obispo, Calif. Monthly Weather Rev. 54, 161-163.

Irving, D. 1965 The Destruction of Dresden. New York, NY: Ballantine.

Kerr, J. W. 1971 Historic fire disasters. Fire Res. Abstracts Reviews 13, 1-16.

Lee, S. L. and Hellman, J. M. 1974 Heat and mass transfer in fire research. Advances in Heat Transfer, vol. 10, pp. 219-284. New York, NY: Academic.

Lifton, R. J. 1967 Death in Life -- Survivors of Hiroshima. New York, NY: Random House.

Lohneiss, W. H. 1966 Observations of a fire-generated vortex. Fire Res. Abstracts Reviews 8, 184-187.

Long, R. R. 1967 Fire storms. Fire Res. Abstracts Reviews 9, 53-68.

Lyons, P. R. 1978 Techniques of Fire Photography. Boston, MA: National Fire Protection Association.

Michaud, L. M. 1975 Proposal for the use of a controlled tornado-like vortex to capture the mechanical energy produced in the atmosphere from solar energy. Bull. Amer. Meteorol. Soc. 56, 530-534.

Miller, C. F. 1968 Summary of damage inflicted by air raids on the city of Hamburg in the period July 25 to August 3, 1943. Rept., Proj. MU-6464. Menlo Park, CA: Stanford Research Institute.

Morton, B. R. 1959 Forced plumes. J. Fluid Mech. 5, 151-163.

Morton, B. R. 1970 The physics of fire whirls. Fire Res. Abstracts Reviews 12, 1-19.

Morton, B. R., Taylor, G., and Turner, J. S. 1956 Turbulent gravitational convection from maintained and instantaneous sources. Proc. Roy. Soc. A234, 1-23.

Murgai, M. P. 1976 Natural Convection from Combustion Sources. New Delhi, India: Oxford & IBH.

Pirsko, A. R., Serguis, L. M., and Hickerson, C. W. 1965 Causes and behavior of a tornadic fire-whirlwind. Res. note PSW-61. Berkeley, CA: Pacific SW Forest and Range Exp. Station.

Rodden, R. M., John, F. I., and Laurino, R. 1965 Exploratory analysis of fire storms. Rept., Project MU-5070. Menlo Park, CA: Stanford Res. Inst.

Rotty, R. M. 1974 Waste heat disposal from nuclear power plants. Tech. memo. ERL ARL-47, Air Resources Lab., Environmental Res. Labs. Silver Spring, MD: National Oceanic and Atmospheric Adm.

Schubert, R. 1969 Examination of the building density and fuel loading in the districts Eimsbüttel and Hammerbrook in the city of Hamburg as of July 1943. Translation, Project MU-6464. Menlo Park, CA: Stanford Research Institute.

Shapley, D. 1972 Technology in Vietnam: firestorm project fizzled out. Science 177, 239-241.

SIPRI (Stockholm International Peace Research Institute) 1975 Incendiary Weapons. Cambridge, MA: MIT.

SIPRI (Stockholm International Peace Research Institute) 1977 Weapons of Mass Destruction and the Environment. New York, NY: Crane, Russak.

Smith, R. K., Morton, B. R., and Leslie, L. M. 1975 The role of dynamic pressure in generating fire wind. J. Fluid Mech. 68, 1-19.

Taylor, R. J., Evans, S. T., King, N. K., Stephens, E. T., Packham, D. K., and Vines, R. G. 1973 Convective activity above a large-scale bushfire. J. Appl. Meteorol. 12, 1144-1150.

Taylor, D. F. and Williams, D. T. 1968 Severe storm features of a wildfire. Agricultural Meteorol. 5, 311-318.

Thomas, G. and Witts, M. M. 1977 Enola Gay. New York, NY: Stein and Day.

Thorarinsson, S. 1966 Surtsey, the New Island in the North Atlantic. Reykjavik, Iceland: Almenna Bokafelagio.

Thorarinsson, S. and Vonnegut, B. 1964 Whirlwinds produced by the eruption of Surtsey volcano. Bull. Amer. Meteorol. Soc. 45, 440-444.

Ying, S.-J. 1965 The fire whirl. Tech. rept., Engng. Sci. Lab., Div. Engng. and Applied Phys. Cambridge, MA: Harvard U.

TABLE 1. RESULTS OF PARAMETRIC VARIATION

CASE	QUANTITY TIME (h) UNIT	$z_{\overline{f}}$ 0 km	$z_{\overline{f}}$ 4.8 km	B all m/s^2	W(0) all m/s	W_{max} 4.8 m/s	$z(W_{max})$ 4.8 m/s	V_{max} 4.8 m/s	$z\|_{\overline{f}=0}$ 0.0 km	$z\|_{\overline{f}=0}$ 4.8 km	t_{rise} 0.0 s	t_{rise} 3.0 s
NOMINAL		3.94	7.14	0.246	25.6	49.3	1.90	2.56	2.80	4.80	80.0	92.2
C = 50		3.94	5.66	0.246	25.6	42.5	1.38	2.72	2.80	4.38	80.0	94.4
C = 200		3.94	6.47	0.246	25.6	56.9	2.38	2.42	2.80	5.15	80.0	86.6
$\epsilon = 2 \cdot 10^{10}$		4.89	8.16	0.246	32.2	72.8	2.82	2.97	3.48	6.59	106.5	107.6
$\kappa = 0.95$, $\overline{V}_0 = 0.45$		2.53	3.23	0.614	25.6	35.2	0.72	3.04	1.70	2.36	40.6	44.8
$b = 0.5$, $\overline{V}_0 = 0.35$		2.02	2.38	0.246	15.0	16.0	0.62	1.73	0.77	0.87	56.3	67.4
$\overline{T}(\overline{z}) = 1.8$, $\overline{V}_0 = 1.1$		4.21	5.63	0.246	25.6	45.0	1.60	4.53	2.80	4.40	413.0	444.0
$\overline{T}(\overline{z}) = 3.6$, $\overline{V}_0 = 1.6$		4.81	5.81	0.246	25.6	44.3	1.50	6.33	2.80	4.36	1057.0	958.0

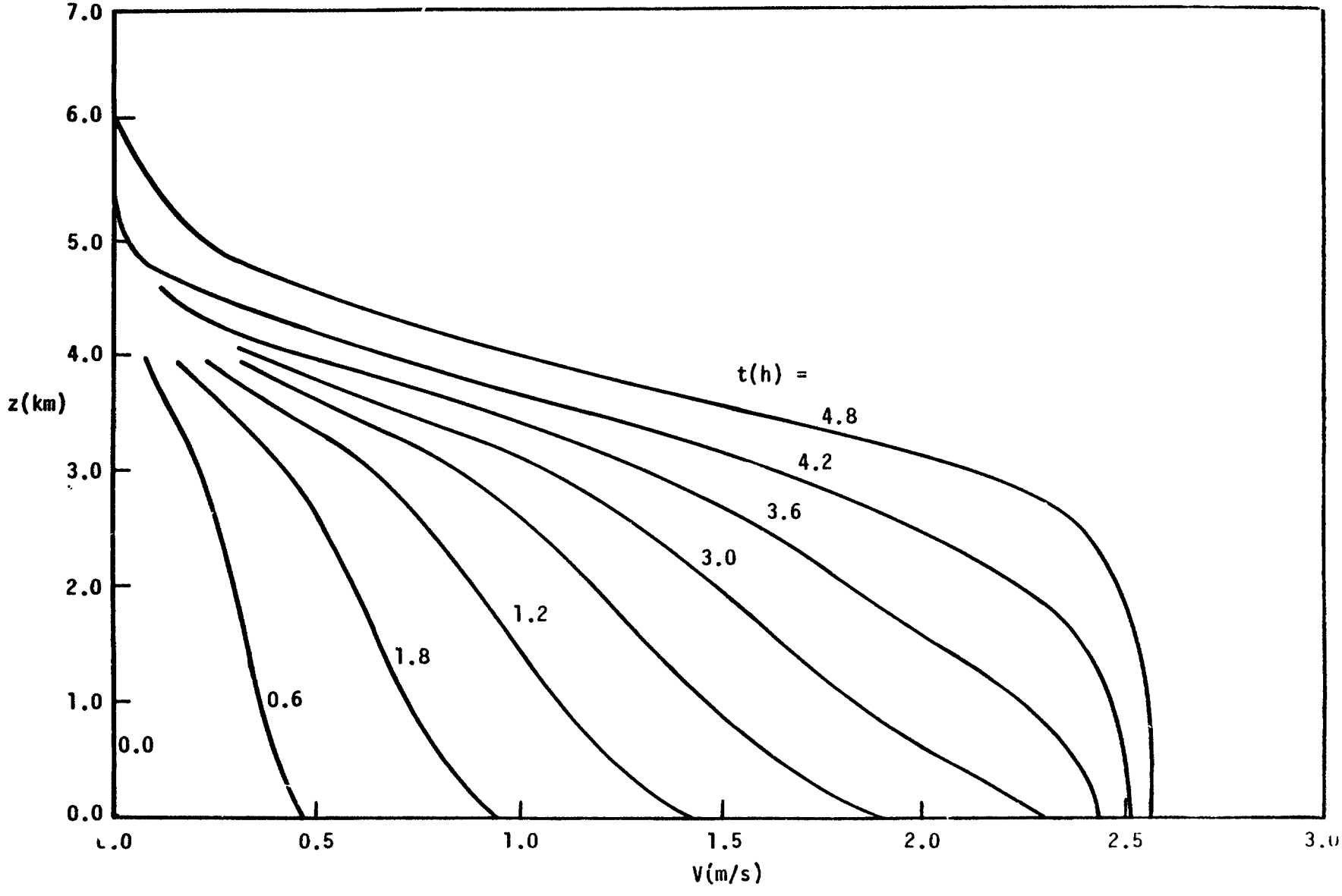

Figure 1. The swirl speed V is presented as a function of altitude at various times for the nominal case. At t = 0, the initial swirl speed V = 0 from z = 0 to the top of the column at z = 3.94 km.

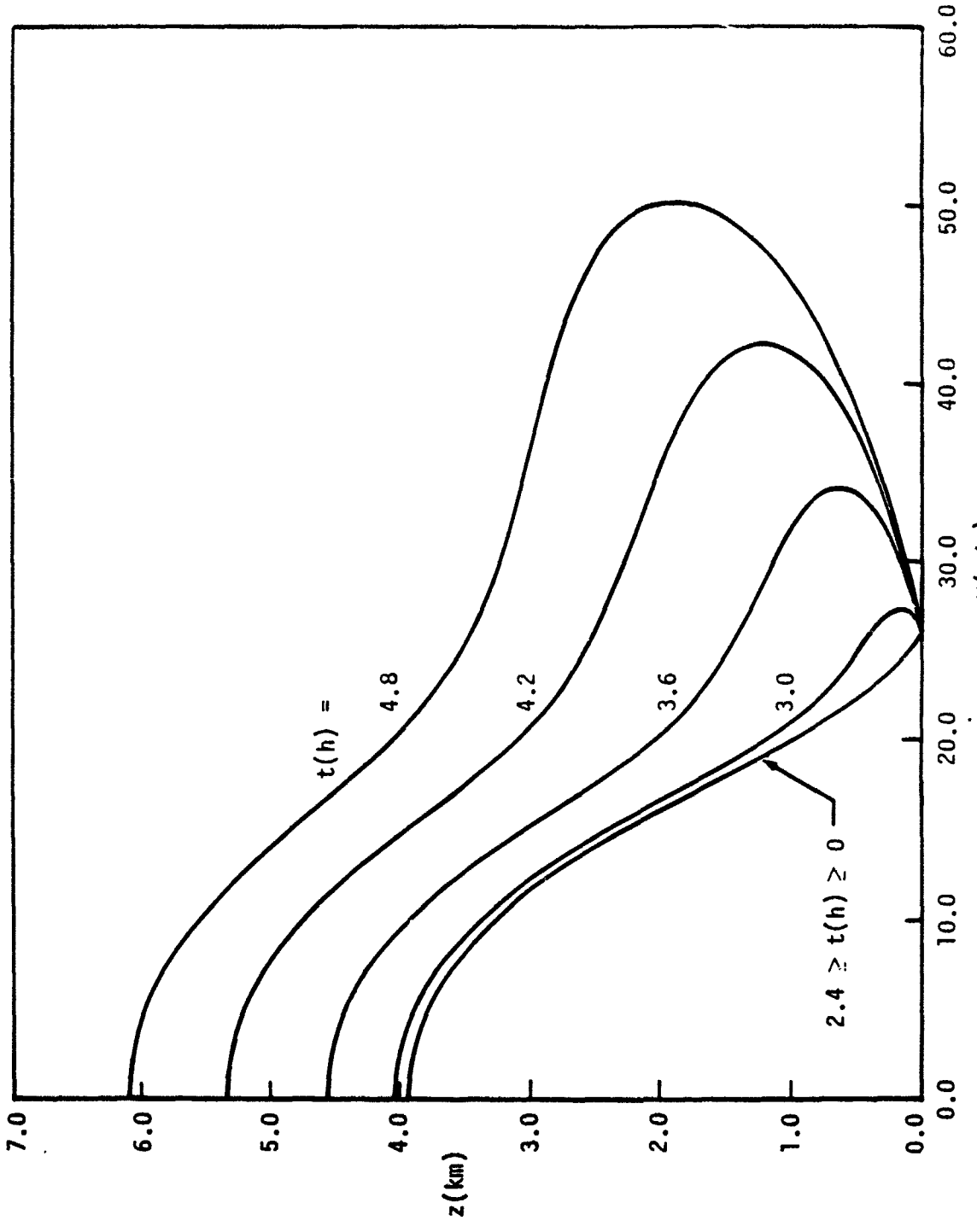

Figure 2. The updraft speed W is presented as a function of altitude at various times for the nominal case.

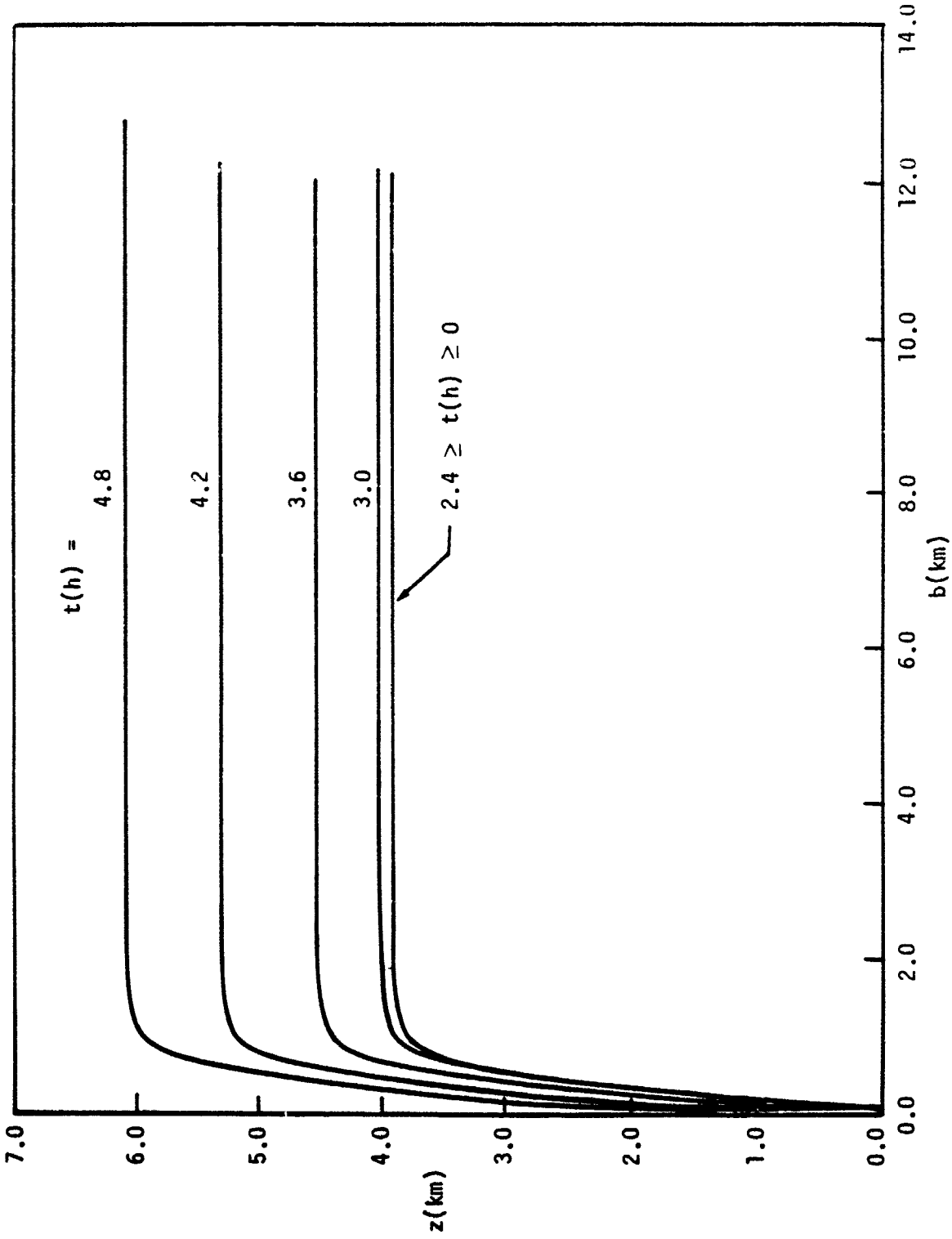

Figure 3. The plume width b is presented as a function of altitude at various times for the nominal case.

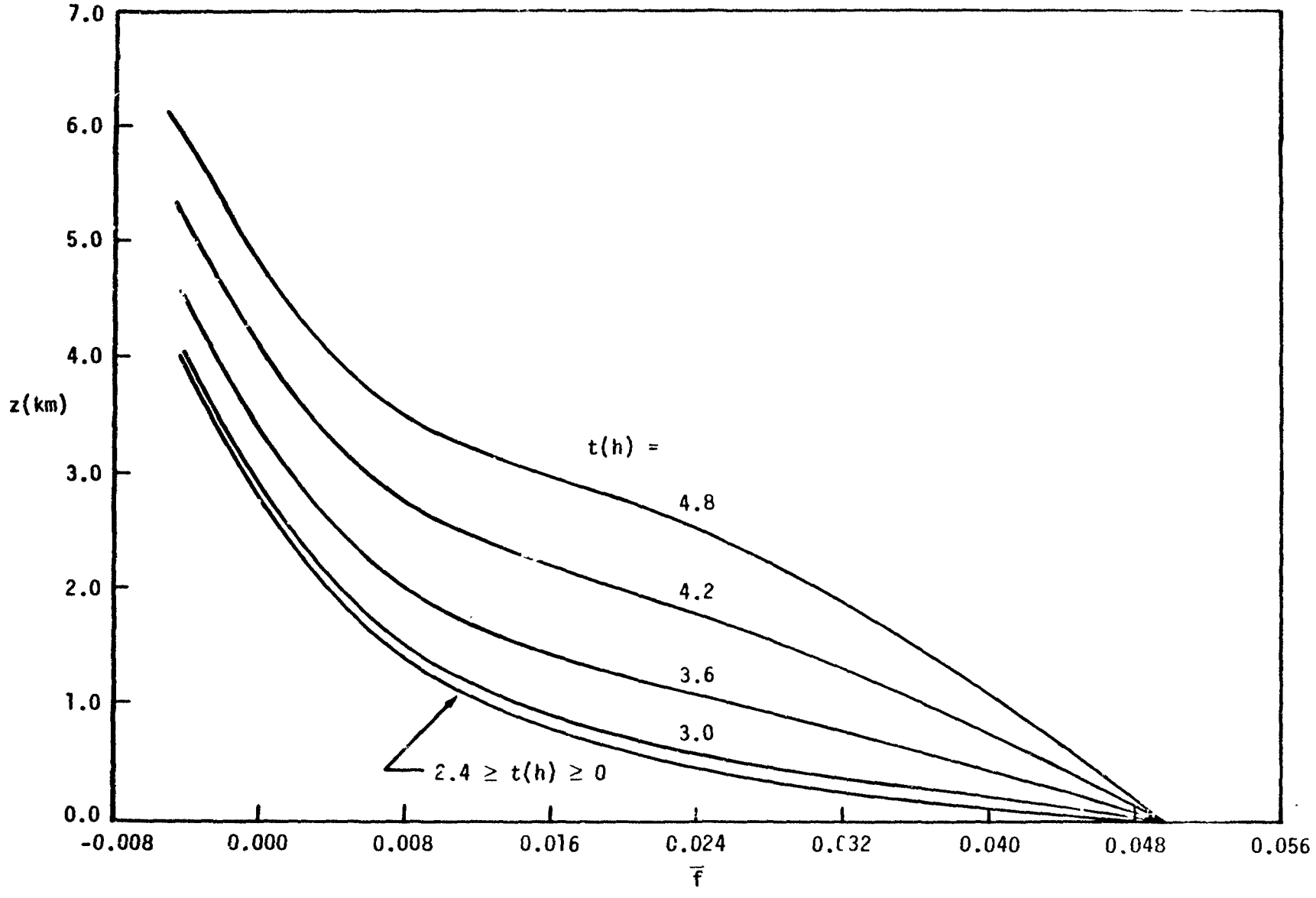

Figure 4. The dimensionless density discrepancy $\bar{f}$ is presented as a function of altitude at various times for the nominal case.

DISTRIBUTION LIST

DEPARTMENT OF DEFENSE

Defense Intelligence Agency
ATTN: DB-4C2, C. Wiehle

Field Command
Defense Nuclear Agency
ATTN: FCTXE
ATTN: FCTT, W. Summa
ATTN: FCTT, G. Ganong

Defense Technical Information Ctr
12 cy ATTN: DD

Defense Nuclear Agency
ATTN: SPTD, Frankel
4 cy ATTN: TITL

OTHER GOVERNMENT AGENCIES

Department of Commerce
Center for Fire Research
ATTN: R. Levine

US Forest Service
ATTN: C. Chandler

Federal Emergency Management Agency
ATTN: Asst Assoc Dir for Rsch, J. Kerr
ATTN: Ofc of Rsch/NP, D. Bensen

Office of Emergency Svcs
ATTN: W. Tonguet

FOREIGN AGENCIES

Fire Research Establishment
ATTN: Dr P. Thomas

The Swedish Fire Research Bd
ATTN: V. Sjolin

DEPARTMENT OF ENERGY CONTRACTORS

University of California
Lawrence Livermore National Lab
ATTN: B. Bowman
ATTN: B. Hickman

Los Alamos National Lab
ATTN: J. Chapiak
ATTN: Dr D. Cagliostro

DEPARTMENT OF DEFENSE CONTRACTORS

California Research & Technology, Inc
ATTN: Rosenblatt

Center for Planning & Rsch, Inc
ATTN: J. Rempel
ATTN: R. Laurino

Charles Scawthorn
ATTN: C. Scawthorn

Harvard University
ATTN: Prof C. Carrier

DEPARTMENT OF DEFENSE CONTRACTORS (Continued)

Institute for Defense Analyses
ATTN: L. Schmidt

Management Science Associates
ATTN: K. Kaplan

Mission Research Corp
Attention Sec Ofc for
ATTN: J. Ball
ATTN: J. Sanderlin

Modeling System, Inc
ATTN: G. Berlin

University of Notre Dame Du Lac
ATTN: A. Murty Kanury

Pacific-Sierra Research Corp
ATTN: H. Brode, Chairman SAGE
ATTN: R. Small
ATTN: D. Larsen

R&D Associates
ATTN: D. Holliday
ATTN: J. Carpenter
ATTN: R. Port

Research Triangle Institute
ATTN: R. Frank

Science Applications, Inc
ATTN: D. Groce
ATTN: M. McKay
ATTN: M. Drake

Science Applications, Inc
ATTN: J. Cockayne

Scientific Svcs, Inc
ATTN: C. Wilson

SRI International
ATTN: T. Goodale
ATTN: J. Backovsky
ATTN: S. Martin
ATTN: R. McKee

TRW Electronics & Defense Sector
4 cy ATTN: F. Fendell
4 cy ATTN: G. Carrier
4 cy ATTN: P. Feldman

IIT Research Institute
ATTN: H. Napadensky
ATTN: T. Waterman

Physical Dynamics, Inc
ATTN: W. Kreiss
ATTN: B. Freeman

Los Alamos Technical Associates, Inc
ATTN: P. Hughes